

5 Dear Dr. Fennel

Please find attached revised manuscript and responses to reviewers. We have carefully revised manuscript according to the comments of two reviewers. We think manuscript has improved thanks for the suggestions. Please note that we have:

- 10
- changed the manuscript title to: “Wind-driven stratification patterns and dissolved oxygen depletion off the Changjiang (Yangtze) Estuary” according to the suggestion of first reviewer.
 - added another co-author (Dinghui Shang) due to implementing Chl *a* data to the manuscript (as suggested by first reviewer).

Best Regards,

15 Taavi Liblik

Responses to reviews and manuscript file (with track changes)

20 **Responses to reviewer 1 – Fabian Große**

Reply: Thank you for your careful reading and comprehensive review! Manuscript has been improved thanks for your suggestions/comments. We have taken into account most of your comments in revising the manuscript. Please notice that in the replies we provide texts from the draft of revised paper. There might be minor changes (related to language) in the final revised paper submission.

30 Comment: However, my major issue with the manuscript at hand is that it is often hard to get what findings are based on what results (due to a lack of figure description and cross-referencing). This leaves me with the impression some of the figures are unnecessary and should be removed. In consequence, the conclusions appear a bit limited and more of a summary of what has been done despite this relatively large number of figures.

35 Apart from that, the manuscript almost exclusively considers and discusses the physical controls of hypoxia, although it is shown by earlier studies and the one at hand that the physical environment (i.e. stratification, which limits DO supply from oxygenated surface waters to deeper layers) only provides the frame for hypoxia. DO consumption (represented by AOU in this manuscript), driven by primary production and subsequent organic matter degradation, is required for its formation. The described upwelling plays an essential role for enhancing primary production (and subsequent DO consumption), yet this is barely mentioned.

40 Therefore, I recommend reconsidering the manuscript for publication after major revisions. For specific comments and suggestions please see below.

45 Reply: We agree with the critics on referencing and description of figures and we have dealt with the issue.

We also agree conclusions needed rewriting.

Yes, this is true, we focus on physical processes impacting hypoxia. We believe, the physical environment and its sensitivity to forcing is extremely important for hypoxia formation here.

50 Stratification is just one, but not only aspect. Advection of the diluted water is driven by
physical processes, as well is deep water intrusion. Both are required for the existence of
hypoxia and both depending on wind forcing. Of course oxygen consumption is required to
have hypoxia, but advection and diffusion are important as well in oxygen budget. Likewise,
55 it is important, where all this oxygen consumption driven by primary production happens.
Latter is driven by physical forcing. We agree DO consumption and related processes must be
more highlighted in this paper. But the focus of the paper stays as it was.

Action: In the revised manuscript citing and description of figures is much more
comprehensive. Fixing has been done in the entire manuscript, particularly in the results
60 section. Figures were cited 53 times in the original manuscript, and now reaching 152 times in
the revised document.
We have rewritten conclusions according to your specific comments.

We have improved introduction to show the focus of the paper more clearly. Primary
65 production and consequent organic matter in the context of consumption is now much more
highlighted in the manuscript, particularly in introduction and discussion. Likewise we
mention this now in results and conclusions. We have added chl-a maps to give background
information about the initial causes of consumption, but we keep our focus on wind forcing
and related effects on oxygen fields. Otherwise we rely on existing papers, which have dealt
70 with biogeochemical processes and have shown well the importance of the CDW and
upwelling on oxygen consumption in this region.

75 **General comments**

Comment: A large fraction of the figures are not (explicitly) used/described in the Results
section, which in parts makes it difficult to follow. In most cases, it is not stated why a
specific figure is shown. For instance, what is the purpose of comparing satellite sea surface
80 salinity (SSS) with the mooring time series (Fig. 2), while the mooring data is not used in the
rest of the manuscript, nor is satellite SSS? Figures 4 and 5 (transects) are not mentioned
explicitly, although they clearly show some important vertical patterns, like the subsurface
hypoxic layer reaching almost up to 5m depth (Fig 5). However, this is only mentioned in the
discussion. Figures 11-13 are also only mentioned in the Discussion, which is too late. All
figures that are relevant for the manuscript need to be described in the Results section in order
85 of their appearance.
Irrelevant figures should be removed. It's hard to tell for me, what figures are really important
because of the partial lack of description; possibly some panels could be removed from Figs.
3-5.

90 Reply: We agree the critics about description of figures and results. Sea surface salinity was
used both in results and discussion part of the manuscript (Fig. 11). We agree, figures 3-5
were not described well enough in detail in the original manuscript. All figures except figure
13 are mentioned in the results.

95 Action: We have extended the manuscript to give much more details about these figures, and
each subplots have been separately cited in the context.
We also considered the suggestion to include figure 13 in results part, but its major content is
very related to earlier studies. Thus, we think it is better to start using it in discussion.
Otherwise citing to figures is more extensive in the revised manuscript.

100

Comment: The AOU figures (although only very briefly discussed) clearly show the important role of DO consumption driven by organic matter degradation for hypoxia formation. However, this factor is only briefly mentioned in both introduction and discussion. Figure 5 shows a distinct increase in AOU in the subsurface from offshore toward the coast. This strong increase indicates that the DO minimum in the near-shore subsurface area is formed via local organic matter remineralisation, although the reduced DO concentrations in the offshore subsurface waters suggest that the water is preconditioned for hypoxia formation. These things should be discussed as well, as the physics alone cannot explain hypoxia formation. If the survey data contain information on variables that can be used as indicators for organic matter production (e.g. chlorophyll-a/fluorescence observations or nutrient concentrations (as an indicator for enhanced nutrient supply via upwelling), I strongly recommend showing results for the indicator variable(s), e.g. as plots of surface concentrations or vertically resolved transects. This would strengthen the results and discussion, and provide a good connection between physical environment, productivity and DO depletion.

Reply: We agree, the background of the do consumption was not well enough mentioned in the previous version of manuscript.

Action: Features in vertical sections are described much more detailed in the revised manuscript. Likewise, information related to consumption is more highlighted in introduction, results, discussion and conclusions. We have added chl-a to the manuscript (to fig. 6) and described it. However, we believe that consumption related processes are quite intensively studied and going deeper into that topic in this paper is out of focus (as wind forcing has been out of focus in many other studies, which have dealt with link between primary production and hypoxia). The preconditioning of offshore water aspect is now included in the discussion.

130

Comment: The conclusion reads as if the key findings are (1) that stratification must be present for hypoxia to form (which is nothing new) and (2) that there are two modes of salinity (i.e. stratification) and DO distribution patterns, which are controlled by the prevailing wind field (which is new). The latter is a very interesting finding, however, in terms of conclusions it would be absolutely worthwhile to raise the implications of this finding, e.g. for survey planning, or even for the potential development of a hypoxia forecasting system.

Reply: Thank you for the good suggestion.

Action: the first point about stratification, this is much more specific in the revised manuscript (mainly because of reviewer 2 comment). It says now "Pycnocline created by Kuroshio subsurface water is precondition and determines where hypoxia could develop". There is much more analysis dealing with this issue thorough results and discussion section in the revised manuscript. Your recommendation for conclusion is included now: "There is a strong connection between the upper boundaries of Kuroshio intrusion and oxygen depletion. The sensibility of the boundaries to wind forcing shapes oxygen conditions considerably in the area. Autonomous measurement campaigns by mooring arrays and underwater gliders could considerably improve the knowledge about related processes. Concepts suggested in the present work can be utilized, when planning in-situ experiments. Wind, river discharge, remotely

150 sensed salinity and altimetry data can be used to forecast hydrographic situation and potentially hypoxic areas prior field works.”

155 Comment: Considering that SSS and wind information can be obtained with relatively high spatio-temporal resolution, a combination of both with the findings of the study could be used to make spatially resolved forecasts on likely occurrences of hypoxia, which in turn could be used to connection between wind field, SSS (or Changjiang Diluted Water) and hypoxia is based on only two years, with some additional support from the literature (see Discussion).
160 However, if the authors were able to match up a few more years of high wind stress (according to their study) with corresponding hypoxia patterns, this could at least point into the right direction and provide directions for useful future research. The authors should furthermore discuss what role the different survey timing played for the differences in the observed features as the 2017 survey took place at the beginning of the winter monsoon, while the 2015 one was done in the middle of the summer monsoon. This obviously has a
165 strong effect on the wind field.

Reply: Thank you for good suggestions.

Action: We have added more literature examples to discussion. And we have added a subsection to the discussion about survey planning.

170 “Thus, when planning hypoxia related measurement campaigns in future, it is worthwhile to take into account wind-driven transport, river discharge, remotely sensed salinity and altimetry to forecast spreading of the CDW, upwelling occurrence and deep water intrusion and according to latter factors estimate potential hypoxic area prior to field works. This could allow more efficient use of ship time and more detailed sampling of the hypoxic area. ”

175 Yes, timing is important. In the original manuscript, the first section of discussion was initiated by the timing question. But somehow the most obvious fact (which you mention) we did not say out. It has been made in the revised manuscript. In short, timing matters, but the wind conditions in 2015 were not only related to the beginning of winter monsoon (you have
180 mixed years in your comment), but the whole summer stands out times-series (Fig. 12) as with weak summer monsoon. This reveals also in Fig. 11, where we show the occurrence of CDW (by remotely sensed salinity). As a result hypoxia developed in south. We have added an additional reference, where the surveys were also from July and October in 2015. There was more oxygen depletion in north in July, but not hypoxia and very strong hypoxia in south
185 in October.

We have added “Thus, our observations conducted in late August - early September 2015 and late July 2017 illustrate the annual cycle of forcing and latter reflect in oxygen and stratification patterns. On the other hand summer monsoon and river discharge were close to average in the whole summer of 2017 while the summer monsoon was clearly weaker in 2015
190 (Fig. 13a-b). Thus, our observations reflect also the differences in forcing and concurrently the DO distributions between two summers.”

And

195 “It is clear from fig. 11 that CDW transport offshore (to northeast) has occurred in all years, including 2015. However, one can see how year 2015 differs with low value in the inter-annual time series of wind stress of $\tau_c \geq 0.02 \text{ N m}^{-2}$ (Fig. 13a-b) and with considerable southward advection of the CDW (Fig. 11). Monthly mappings of bottom oxygen in 2015 (Li et al., 2018b) does not show significant oxygen depletion in north in any month while deteriorated hypoxia (comparing to our observations) occurred in October.”

200

Comment: Figures: Many figures are not legible in grey-scale, i.e. for colorblind people. I strongly recommend using perceptually uniform color scales, which are available for R, MatLab and Python (and other languages; e.g. <https://github.com/matplotlib/cmocool>). Color references in figure captions should be avoided for the exact same reason. All figure captions must state clearly what data is shown (e.g. over what period they were averaged etc.)

205

Reply: Thank you for bringing this up.

210

Action: We changed figures according to your suggestions.

Specific comments

Comment: Title: I suggest removing “in the area”

215

Reply: Good idea.

Action: Done.

220

Comment: Abstract: The abstract should be rewritten, such that the key messages can be understood without reading the entire manuscript. At this point, it is unclear what the “interaction zone” (line25) between upwelling and surface freshwater is meant to be. High AOU furthermore does not necessarily mean “high DO utilization there” (i.e. local consumption; line 24), especially in the case of advected/upwelled subsurface waters, which are likely to be already undersaturated in DO. Discuss the findings chronologically (first 2015, then 2017).

225

Reply: We agree.

230

Action: We have re-written the abstract. We realized interaction as such is indeed not analysed and is not under focus of the present study. We removed it from abstract. The abstract has now been written in chronological order.

235

Comment: Lines 50/51: nutrients lead to production, which in turn leads to sinking/sedimentation of organic matter. This is an important aspect, which should also be more emphasized in the discussion (and the results, if possible with the survey data; see my general comment).

Reply: We agree this is important aspect.

240

Action: We have emphasized this topic more comprehensively in introduction of the revised version of the manuscript. Likewise, we have extended the topic in the discussion. We have included Chl a data to the results section. We also mention primary production in conclusions in the revised paper.

245

Comment: Lines 92-94: Again, what about the influence on productivity? Upwelling brings nutrients into the euphotic zone, significantly enhancing organic matter production.

250 Reply: I am not 100% sure, if I understand your concern about lines 92-94 (there is no upwelling mentioned). Nevertheless, I understand your general concern.

255 Action: In the revised manuscript, we have described the role of productivity in the CDW and due to upwelling and the consequences to oxygen depletion more thoroughly. Also we have made more clear, what is the focus of our work. We believe after these changes it is understandable for a reader why we write lines 92-94 like this.

Comment: Lines 99-101: I would remove this paragraph.

260 Reply: We removed.

265 Comment: Line 109: There is a 1-month difference in the survey timing between the two years. It would be nice to include a statement in the discussion to what extent relates to the seasonality in the monsoon cycle and if/how it affected the differences between the observations in both years.

Reply: Yes, we agree. This topic was dealt in the first section of the discussion (original manuscript) but clear statement about the matter was missing.

270 Action: We extended there: "Both, maximum frequency of southerly wind and river discharge in the annual cycle occur in July-August (Figs. 13a,c). Thus, our observations conducted in late August - early September 2015 and late July 2017 illustrate the annual cycle of forcing and latter reflect in oxygen and stratification patterns."

275 But we also need add: "On the other hand summer monsoon and river discharge were close to average in the whole summer of 2017 while the summer monsoon was clearly weaker in 2015 (Fig. 13a-b). Thus, our observations reflect also the differences in forcing and concurrently the DO distributions between two summers. "

Comment: Line 110: state the number of stations you used for both years

280 Reply and action: We added (65 in 2015 and 49 in 2017).

285 Comment: Lines 119-121: Since you do not describe Fig. 11 (until the discussion), do you need to show/discuss it at all? If not, remove the description of the satellite product and Figs. 2 and 11. If you need it, what is the spatial resolution of the satellite product and how does it match in-situ spatial patterns observed during the survey?

290 Reply: We checked again and found that we have described and cited Fig. 11 under the results section, please see 295-302 (original submission). Resolution is 0.25°.

Action: We need to show and discuss figure 11. We considered merging of the Fig. 11 related text from discussion to results. But we realized this text (though have some results) has many discussion elements. So we prefer to keep it there. However, we added text after the section we just mentioned (295-302, original submission). We introduce there also 2016/18 sea surface salinity observations (CDW spreading).

295 We added information about resolution to data and methods section. Match between satellite and in-situ salinity is quite good. We don't want to add another figure just for comparison. Time-series comparison (Fig. 2) shows well that remotely sensed salinity is useful product in

300 this region. We think fig. 2 is a good indicator of remotely sensed salinity quality in this area
also for further studies. There are very limited time-series available in this region.

Comment: Figure 1: The labels of transects S15/S17 are barely visible. Remove color references in caption.

305 Reply and action: Done

Comment: Lines 122-128: Is the used wind forcing the same that the GLORYS model uses? Please specify. If it's not, I advise using the same one.

310 Reply: It is not exactly the same. GLORYS uses ERA-Interim wind. For the wind forcing we
use the dedicated CMEMS Wind product, which uses remote sensing observations from
several satellite missions. However, potential temporal gaps in the observational time-series
are filled by ERA-interim. The product has been validated and the quality is well proven the
according to the public documents provided by CMEMS.

315 Action: We prefer to keep wind forcing as it is now.

Comment: Lines 132/133: This is a result and should be stated in the Results section. Where
is that shown? Include reference to corresponding figure.

320 Reply: We agree, it was repeating of results.

Action: We removed it from here. We state this also in results section and cite to figure 8
(simulated currents) and 3 (observed salinity).

325 Comment: Lines 134-142: Please state why you are analyzing AOU. E.g. to illustrate the role
of DO consumption.

Reply and action: We added suggested sentence.

330 Comment: For the entire section: please refer to figures and figure panels where appropriate.
Right now it's really hard to know what figure (panel) to look at due to minimal cross-
referencing.

335 Reply: We agree.

Action: We have increased number of references to figures considerably. We cite to panels.

340 Comment: Lines 151/152: Please state why you analyse the spatial patterns (e.g. to put the
DO observations in context with the physical environment).

Reply: We agree.

345 Action: We added to the very beginning: "In order to link the thermohaline structure and DO
observations we next analyze temperature.."

350 Comment: Line 154 and Fig. 3: In the figure, you show the 31 isohaline, here you refer to the 30 isohaline.
Please be consistent. I suggest using the 30 isohaline in the figure.

Reply: We fixed.

355 Action: There are 30 both in the figure and text of the revised manuscript.

Comment: Lines 164-168: You “describe” 3 figures on 5 lines. It is not possible to understand what finding is based on what figure. It also gives the impression that 1-2 of the figures are superfluous.

360 Reply: We agree with critics.

Action: We have solved this issue. Figures are now cited by subplots. Also more text is added to describe the results more comprehensively.

365 Comment: Figures 3-5, 6a-2/b-2: Don’t use the jet color scale, dark red and dark blue are indistinguishable in grey scale (i.e. for colorblind people). Use standard panel labels, i.e. a, b, c, d etc. (not a-1, a-2, b-1, b-2, ...)

370 Reply: We changed.

Action: We changed colorscale and changed panel labels according to your suggestion.

375 Comment: Lines 190-192: Upwelling creates favourable conditions for organic matter production (primary production), which then drives DO consumption. You should not skip this process. If you have chlorophyll (or nutrient) data, you should show them to illustrate this.

Reply: We made changes accordingly.

380 Action: We have added more text on that topic. We have added chl-a to illustrate the process. Revised text is: “This indicates that coupling between coastal upwelling, which bring subsurface water to shallower depths (euphotic zone) and fresher riverine surface water, created favorable conditions for the primary production in the upper layer and concurrent DO consumption and depletion in the deep layer (Figs. 5h,i,k,l). Higher Chl *a* concentrations in the upwelling areas revealed from the satellite image, although not as high as in north (Fig. 6d)”

390 Comment: Line 195: What do you mean with “a certain physical property of water”? Do you mean temperature or salinity or else? Please specify.

Reply: We specified.

Action: We added: “, e.g. to a temperature-, salinity- or density isohaline.”

395 Comment: Lines 196-199: How did you determine the 2 mg/L AOU-cline to be the “oxycline”? And why do you use the AOU isohaline to define your oxycline and not oxygen in the first place? An oxycline is defined by a strong gradient in DO, not by AOU and not by DO

400 depletion (and you are not using a gradient either), so the term cannot be used here. The 2
mg/L AOU isoline further doesn't seem to match the oxycline nor the upper boundary of DO
depletion in 2015 (Fig. 4). And what is your basis for using the 24.5°C isotherm to represent
the thermocline? A thermocline is also defined by a gradient in temperature, not by a fixed
temperature; it doesn't seem to represent the thermocline at transect N15 (Fig. 4). I suggest
405 calculating the pycnocline/oxycline using a gradient approach (e.g. strongest vertical
density/DO gradients), which would be much more objective than just picking some isolines.
If they still match (which I expect being the case), this would strengthen your statement that
the pycnocline determines the upper limit of DO depletion (although this is not really new).

Reply: Yes we agree in that, thermocline and oxycline are not the best terms. The reason why
410 the gradient approach (what you suggest) was not used and why we still don't want to use it,
is the fact that if there is upwelling event (like in 2017), then the gradient approach fails. We
would like to show surfacing of the both isolines. Gradient approach does not allow that.
Likewise, gradient approach has some other problems (e.g. small intrusions, which are not
interests of the present study, cause jumps in space). I (T. Liblik) have dealt with this issue on
415 35 sections measured across the Gulf of Finland
(<http://www.borenv.net/BER/pdfs/ber22/ber22-027-047-Liblik.pdf>). For similar reasons we
did not use finally the gradient approach, but used isolines (which varied for every section
though) in that study.

420 Action: We rephrased the terms accordingly, so we don't call the isolines anymore as
thermocline and oxycline. We have changed that in the whole manuscript. 24.5° describes the
upper boundary of the colder water mass (Kuroshio intrusion) while the 2 mg/l AOU
describes the upper boundary of oxygen depletion. This is done in the whole manuscript. In
relation to the comment of other reviewer we now put much more attention to these
425 boundaries in the whole manuscript. It also means that we don't talk about stratification in
general way anymore (as in the original manuscript). We have also added altimetry data
(mean sea level anomaly) to confirm the upwelling/downwelling pattern and related changes
with isolines. We copy here section from the draft of the revised paper to illustrate the
approach/conclusion in the revised paper: " Two features must be present for hypoxia
430 formation: 1) KSSW, 2) CDW and/or subsurface water upwelling. We can conclude that
colder KSSW determines where (including in what depths) hypoxia could develop. Thus,
latter provides necessary precondition for hypoxia. The CDW spreading and/or subsurface
water upwelling (and related biogeochemical, biological processes) determine the magnitude,
exact location and timing of oxygen depletion."
435

Comment: Lines 200-208: I wonder if Fig. 7 adds a lot of information that cannot be obtained
from Figs. 4 and 5? The spatial gradients of thermocline depth indicate the strength of
upwelling, which
440 can be described using the transects. Same applies to the statement on AOU and the effect of
the thickness of the hypoxic layer vs. the DO concentrations. Although I am not sure why this
statement is important? In addition, both factors determine AOU and, at transect C15, a thick
DO depleted layer coincides with very low DO concentrations, which makes it difficult to
quantify what factor is more relevant. I suggest removing this last statement, otherwise the
445 contributions need to be quantified (which does not add to the story).

Reply: We think figure 7 is necessary. In figures 4-5 we have selected 3 sections (not all the
stations) while here we use all the available stations. It gives the better view about lateral

450 isoline distributions, which is hard to visualize just by selected sections. After revision this
figure became even more important. It describes the role of Kuroshio subsurface water as
precondition for the hypoxia (as suggested by reviewer 2).
The statement is related to the fact that if we compare 2015/2017 south/north bottom oxygen,
we get that northern areas was much more oxygen depleted in 2017. However if we compare
455 the total AOU (which describes the oxygen depletion in the whole water column) the two
areas/years have similar values. This means bottom oxygen maps, which is the most common
way to illustrate oxygen problem in this region, not necessarily describe the oxygen problem
(depletion) solely. Other stratification characteristics matter also, not only the strength of the
stratification. We think it is needed to highlight this point for further studies, because oxygen
depletion (Oxygen Dept) is one of the indicator of eutrophication (e.g.
460 <https://www.frontiersin.org/articles/10.3389/fmars.2019.00054/full>).
Yes, that is good point about AOU-layer thickness statement. We have made error with the
statement.

Action: We have added sentence about this matter to discussion, where we talk about
465 importance of vertical location and movements of pycnocline (line 409, original submission).
We rephrased the statement: "It means that high total AOU there (comparing to neighboring
areas) was related both to the thick subsurface DO depleted layer and to the higher
(comparing to surrounding area) AOU." The point we wanted to make is that thickness also
matters. It is often missed, because not full resolution CTD-profiles are used, but bottle values
470 (surface and bottom) instead. PS. This is another reason why want to show fig. 7.

Comment: Lines 243-246: Please provide the equation you use to do this calculation.

475 Reply: We added.

Action: We have added the equation to data and methods.

480 Comment: Lines 249-254: Here, you possibly could mention the monsoon cycle (in relation to
the differences in survey timing) as the 2015 survey took place at the end (beginning) of the
summer (winter) monsoon. Then you could also be a more specific with respect to your
hypothesis on the main cause for the 2015 vs. 2017 differences.

485 Reply: Yes, this can be already mentioned here.

Action: Added "Since our surveys are conducted annually one month apart, the differences
between the two surveys might be associated with the annual cycle in wind climate and river
discharge. Our hypothesis is that the dominant factors behind the discrepancy of the two
surveys are wind forcing and river discharge, and possibly their seasonality."

490 Comment: Lines 256: Does Fig. 8 show wind and currents averaged over the 7-day periods
before the surveys or the only averaged over the single day 7 days before the surveys? Please
clarify and also clarify in the figure caption. If it's averaged over the single day only, why do
you use that one and not the 7-day averages?

495 Reply: We use 7-day averages.

Action: We changed the sentence “Mean wind, surface currents and bottom currents during 7 days prior to the surveys are presented in Fig. 8.” and figure caption accordingly.

500

Comment: Lines 268-270: Is this sentence relevant? Does the negligible bottom current have an important effect on the observed patterns? If yes, clarify. By talking about a buoyant current you also imply that it’s baroclinic.

505 Reply: We agree, indeed the sentence can be omitted.

Action: We removed it.

510 Comment: Lines 271-277: Did you calculate the mean winds at the same location as the currents? Please clarify. Further state which different wind directions you used to calculate correlations and to determine the best one. Possibly state the highest values of the other correlations, too, in order to illustrate the difference between the SE-NW direction and the others.

515 Reply: Not in the same location. For all the work one location was used for the wind. We calculated all directions by 10 degree step. We believe giving correlation values of other directions is not necessary. It is higher closer to the best direction (near SE-NW) and it is weakest across the best direction (NE-SW) as expected. We have tried also to use wind over larger area when preparing manuscript, but it did not give any advantage.

520

Action: We added to the text. “(see the location in Fig. 1)”.
We added to the text “...from different directions (full circle by 10° steps).”

525 Comment: Lines 303-305: I am not sure I understand this statement. You define wind velocity intervals of 0.25 m/s width and average the corresponding current velocities simulated by the model, right? Perhaps you can explain this more clearly. Also, do you do this for every model grid cell in the area of interest or just for the location marked in Fig. 8?

Reply: Yes, it is done as you wrote. We do it for the location marked in Fig. 8.

530

Action: We tried to rephrase “We grouped the simulated v_m to the wind velocity w_c classes with step of 0.25 ms^{-1} and took average of the each group. By doing this, we found relation between mean w_c and v_m .” We hope it is clearer now.
We added information to the previous sentence to make it clear: Next we make an attempt to quantify the two CDW spreading cases caused by wind forcing through analyzing meridional currents v_m at section S1 (see Fig. 8) and wind data from the period June–September in 1993-2018.”

535

540 Discussion:

Comment: Lines 335-338: You refer to Ekman transport, yet you do not show any analysis of it. You do show near-surface currents (0-5 m depth; Fig. 8), however, the Ekman depth (over which you would need to average/integrate to get Ekman transport) is likely deeper than 5 m and will vary depending on the wind speed. It would indeed be nice if you showed the Ekman velocities in order to illustrate the upwelling conditions.

545

Reply: We have made mistake there, what we meant is Ekman surface current.

Action: We fixed the error.

550

Comment: Lines 339-355: Figures 11-13 have not been mentioned before here; you need to do this in the Results section. It is not possible to follow this discussion without prior description of these results. I also do not see the benefit of discussing 2016 since you do not provide information on the DO conditions in that year. The last sentence in this paragraph is entirely speculative, unless you provide information on the DO conditions in 2016 and 2018 (e.g. from other studies if available).

555

Reply: This is not true. Content at section 295-302 (original submission file) is based on Fig. 11 and the figure is mentioned there as well. Same is with the figure 12. It was included in the last section of the results.

560

You are correct about figure 13 – it appears in the discussion first. However, this figure is so much linked to the discussion that it is difficult to handle it before without repeating, which would be annoying for a reader. The annual cycle aspect is now mentioned (as reaction to your other comment) in the results part. So this information is provided now before discussion. We hope discussion is easier to follow after those changes.

565

The last sentence there is speculative indeed. Previously in the results we have linked wind, discharge, CDW spreading and hypoxia in 2015/2017. In the same discussion section we show that wind and discharge qualitatively explain CDW spreading. Naturally, we should discuss/hint at least, how the oxygen picture look like based on this limited information.

570

We have cited to the hypoxia reported in north in 2016 (Zhang et al., 2019), which very well confirm our suggestion.

575

Action: We have extended section in results about Fig. 11 in revision and included some sentences about 2016, 2018 observations there (as reaction to your other specific comment).

The figure 12 is important to show that mean current structure a week before 2015/2017 surveys (Fig. 8) holds truth also when we take historical winds-currents and group them according to our criteria. We have added such explaining sentence about this aspect to the very end of the results.

580

We made the speculative statement softer by replacing “should“ with “could”.

585

Comment: Lines 360-368: This qualitative comparison of the findings of this study with existing literature is very useful and it suggests that the wind stress (in combination with river discharge) could possibly be used for the development of a simple forecast of hypoxia occurrence using remotely sensed SSS and wind information. This could be discussed, although it may need support by more examples than only the few years mentioned. There is some more literature on hypoxia observations in the East China Sea, which the authors may want to check, e.g.:

590

Zhu et al. (2011) <https://doi.org/10.1016/j.marchem.2011.03.005>

Zhu et al. (2017) <https://doi.org/10.1016/j.marpolbul.2017.07.029>

Li et al. (2002) <https://link.springer.com/article/10.1360/02yd9110>

595

If the patterns described in these papers match the “wind-based likelihood” of hypoxia as suggested by this study, the authors could make a case here, which could provide a good direction for future work.

Reply: Thank you for the suggestion.

600

Action: We have added more examples to the suggested section and also to the section before (where we talk about SSS). We also added sentence about synoptic scale variability until the end of the section.

605

End of the section now looks like this “Such situation has been captured for instance in 1998 (Wang and Wang, 2007) and in 1999 (Li et al., 2002). However, on the top of the inter-annual variability and annual cycle are synoptic scale changes of wind-driven currents and river forcing, which likely influence the distributions on shorter time scales (Fig. 10). Thus, when planning hypoxia related measurement campaigns in future, it is worthwhile to take into account wind-driven transport, river discharge, remotely sensed salinity and altimetry to forecast spreading of the CDW, upwelling occurrence and deep water intrusion and according to latter factors estimate potential hypoxic area prior to field works. This could allow more efficient use of ship time and more detailed sampling of the hypoxic area. ”

610

615

Comment: Line 363: “probably occurred” is too speculative. Either you have support for this statement or you should rephrase it, e.g., to “could have occurred”

Reply: We agree.

620

Action: We rephrased as you suggested.

Comment: Lines 377-379: Irrelevant. Remove the whole paragraph

625

Reply: The point we wanted to make here is that in the case of southerly winds CDW might impact surrounding ocean also out from our study area. We believe statement hinting that should stay in manuscript.

630

Action: We rephrased the section. We hope its importance comes out better now. “Offshore, east- or northeastward advected CDW caused by southerly wind, as we observed in 2017, might form detached eddies due to interaction of the Ekman flow and density driven frontal currents (Xuan et al., 2012). Those eddies bring CDW further offshore and alter physical, chemical characteristics (including oxygen conditions) and primary production in the water column (Wei et al., 2017). On the other hand we noted ventilating impact of colder cyclonic eddy in north in 2015.

635

640

Comment: Lines 381/382: The wind-driven near-surface transport offshore is the cause for coastal upwelling of subsurface waters. Please rephrase. The term “upwelling-CDW interaction zone” is not very clear. I understand what you mean, but I would suggest not using this term as it is a bit misleading. The two water masses do not really interact with each other, it is rather a displacement of CDW and its replacement by upwelled water.

645

Reply: Studies in similar environments show that it is not just displacement, but also mixing between two water masses occur (subsurface water and former surface water). E.g. <https://www.sciencedirect.com/science/article/pii/S0278434309002064> found that the share

of former surface was 15% in the formed mixture after upwelling. But we agree, some other term than interaction can be used here.

650

Action: We rephrased “inter-action,” with “coupling,” and added the reference of Wei et al. 2017 who have described the “coupling,” more thoroughly. It now says: “Shoreward, upslope penetration of the sub-thermocline KSSW and hypoxia in the upwelling – CDW coupling zone (Wei et al., 2017a) were observed.”

655

Comment: Lines 386-390: This is one of the few occasions where the role of primary production and nutrient supply is mentioned. This should be expanded and, if possible, strengthened with observations of chlorophyll or phosphate in the Results section.

660

Reply: We agree.

Action: Yes we have expanded the topic and have included chl a for illustration.

665

Comment: Lines 396-397: This could be shown more clearly by drawing oxycline and thermocline in Figs. 4 and 5. I think Fig. 7 is unnecessary.

Reply: Lines can be added, but we would like to keep fig. 7 (we have explained reasons in other answer).

670

Action: We added the lines to the figures 4-5

Comment: Lines 440-444: None of this analysis is shown/described, so it cannot be discussed. If you want to make a statement on potential future changes (or no changes) due to wind, you need to show a figure comparing future wind projections with current winds. Using only one projection from a single model further doesn’t allow for such a strong statement. Please provide references for projected increases in SST and eutrophication if you want to keep the statement.

675

680

Reply: We agree

Action: We removed the section.

685

Comment: The conclusions in general are too weak and rather a summary.
Lines 452-454: Why is the statement on the inclination important?

Reply: Inclination is one reason why northern and southern hypoxia are so different. Deeper clines in south provide more stable and long lasting conditions for hypoxia.

690

Action: We have rewritten conclusions. Inclination as such is not mentioned anymore in conclusions.

Technical corrections

695

Thank you again for the careful look! We have made all the changes you suggested.
Action related your comments is “done” or “solved”.

Regarding your comment:

700 Line 238: what exactly do you mean with river plume **bulge**? It's not clear to me.

Reply: We moved this part to discussion, because the topic is investigated more thoroughly by other papers, no need to repeat.

705 Action: As reaction to your comment we put new sentence there to the beginning: "The faith
of the river plume can be separated to the regions and processes: circulating bulge near the
mouth and downstream current along the coast (Fong and Geyer, 2002; Horner-Devine,
2009). The question is how much of riverine water remains in the river plume bulge and how
much is advected to the neighboring areas. It has been estimated that about 80-90% of the
710 discharge accounts to freshwater transport of coastal current (Li and Rong, 2012; Wu et al.,
2013)."

Responses to reviewer 2

715 Comment: This study addressed two different spatial patterns of hypoxia off the Changjiang Estuary (CE) and discussed the impact of the CDW and wind on hypoxia distributions. But I have two main concerns.

720 Reply: Thank you for reviewing the paper. We have taken both of your main concerns seriously and have made corrections accordingly. Please notice that our replies include preliminary texts from the revised manuscript. We might do small changes in language, in this phase revised manuscript won't be submitted yet.

725 Comment: 1. Observations from 27 August to 5 September in 2015 and from 24 to 29 July in 2017, are actually snapshots in different months and different years. So, their differences result from seasonal or interannual variation or both? In fact, the hypoxia off the CE has prominent seasonal variation and annual cycle, e.g., hypoxia appearing in coastal areas south of the CE in early summer and severe hypoxia in the area north of the CE in August, and also interannual variations (Zhu et al., 2011). 2. The conclusion mentioned that the annual cycle was dominated by wind and the interannual variation by wind and river runoff. But the manuscript did not provide enough evidence for these conclusions.

730 Reply: The annual cycle and inter-annual variability were discussed in the first two sections of the discussion in originally submitted manuscript. In the revised manuscript we have dealt with this question more deeply. Since the 2015 measurements are done one month later in the end of summer, probability of the occurrence of northerly wind is much higher. This is clear from the Fig. 13a. Therefor the snapshot of 2015 describes rather late summer situation and 2017 rather the mid-summer situation indeed. For the inter-annual variability we have analyzed wind and river data (1993-2018) and compared later years with remotely sensed salinity (2015-2018). 735 Mentioned data well agrees with the concept we are suggesting. 2015 distinguishes as special summer in terms of wind forcing and CDW. Weaker summer monsoon resulted in more frequent CDW spreading to the south (as we also observed). Summer 2017 was closer to the "typical" climatological mean summer. We have checked also earlier studies (added more examples during revision, including Zhu et al. 2011) and found similar 740 observations as you mentioned in August. If summer monsoon is at least close to climatological mean, then hypoxia in north is typical. Shortly, our observations somewhat reflect the annual cycle, but 2015 was also special year with weak summer monsoon. We have added also citing to other similar years, when hypoxia in south was observed (Wang and Wang, 2007, Li et al. 1999). 745 The statement in the conclusion you referred was not well worded. We cannot say "Wind forcing and river runoff are main contributors", but we believe we can say based on the study: river runoff and wind are important (not saying it is main) factors in inter-annual and annual cycle of DO.

750 Action: We added following text to the second section of discussion: " Thus, our observations conducted in late August - early September 2015 and late July 2017 illustrate the annual cycle of forcing and latter reflect in oxygen and stratification patterns. On the other hand, summer monsoon and river discharge were close to average in summer 2017 while the summer monsoon was clearly weaker in 2015 (Fig. 13a-b). Thus, our observations reflect also the differences in forcing and concurrently in DO distributions between two summers" 755 and to the fourth section: "However, on the top of the inter-annual variability and annual cycle are synoptic scale changes of wind-driven currents and river forcing, which influence the distributions (Fig. 10). Thus, when planning future hypoxia related measurement campaigns, it is worthwhile to take into account wind-driven transport, river discharge and remotely sensed salinity to forecast spreading of the CDW and potential hypoxic area location prior field works. This could allow more efficient use of ship time and more detailed sampling of the hypoxic area." 760

765 Statement you referred is modified: "Wind forcing and river runoff are important contributors of inter-annual variations and annual cycle, determining the size and location of low DO areas. The DO minimum is located more likely in the northern part in July-August during summer monsoon and in the southern part during rest of the stratified period."

770 Comment: 2. The CE and adjacent area are highly dynamic and complicated, affected by the river plume, the
Yellow Sea Coastal Current, East China Sea Coastal Current, the Taiwan Warm Current and the Kuroshio. The
influence of the intrusion of the TWC and Kuroshio on hypoxia has been discussed previously. But the
manuscript just considered the river runoff and wind, and did not discuss the role of the TWC and Kuroshio. The
775 intrusion can be recognized by the current pattern, bottom salinity and temperature. The authors should analyze
the differences of open ocean intrusion in 2015 and 2017 and their impact on hypoxia distributions.

Reply: Thank you for this comment. We think this suggestion helped to improve the manuscript. Indeed the role
of intrusion was hidden in the manuscript, although we are well aware of intrusion of subthermocline water.

780 Action: We have made changes thorough manuscript to highlight importance of the intrusion. We defined the
upper boundary of the Kuroshio subsurface water mass (as isoline 24.5 temperature) and relate it to the upper
boundary of oxygen depletion (2 mg l⁻¹). This simplification is needed as we don't want to go to fine details of
subsurface water mass formation in this study. The same isolines were used also in the original manuscript, but
785 named as thermocline and oxycline. We believe the terms we use now, are more correct. Our main suggestion is
that position of intrusion is largely related to the wind forcing. Intrusion climbs higher to coastal slope, as
compensation for the offshore transport in the surface layer. And it is located deeper and further offshore, when
there is downwelling with northerly winds. Our second suggestion is that existence of intrusion is necessary
precondition for hypoxia formation. In order to come up with the two suggestions and react to your comment
we:

- 790 (1) described and analyzed both boundaries more deeply in subchapter 3.1. Particularly, the vertical
sections are described more comprehensively in the revised version. 2015 and 2017 are compared in the
context of intrusion there.
- (2) We have added satellite altimetry to give more evidence to our suggestions. The two surveys differ each
795 other clearly by upwelling (2017) and downwelling (2015) and we claim the main reason for this
difference is wind forcing.
- (3) We have highlighted the importance of intrusion, related to oxygen depletion in discussion:
"Importance of KSSW thickness on the oxygen depletion estimations reveal well also if near bottom
oxygen maps are compared with the total AOU maps (Figs. 6g-h). Bottom hypoxia in north in 2017 was
800 much more intense comparing to hypoxia in south in 2015. However, the total AOU was similar in
hypoxic zones in both years due to thicker oxygen depleted layer, i.e. thicker KSSW in south in 2015."
- (4) We have added new section to the discussion highlighting the importance of intrusion. The main point
we make there is that strong stratification strength as such, does not necessarily mean hypoxia. We copy
805 the last part of the section here." Two features must be present for hypoxia formation: 1) KSSW, 2)
CDW and/or subsurface water upwelling. We can conclude that colder KSSW determines where
(including in what depths) hypoxia could develop. Thus, latter provides necessary precondition for
hypoxia. The CDW spreading and/or subsurface water upwelling (and related biogeochemical,
biological processes) determine the magnitude, exact location and timing of oxygen depletion.
- (5) Since in this paper we deal with the position of the intrusion only, we added another section to
810 discussion that mentions other aspects of intrusion: "Besides the barrier effect by creation of the
thermocline, intrusion of KSSW has other implications on oxygen dynamics. First, the subsurface water
is oxygen depleted already before local impact of oxygen consumption. The furthest stations in the
southeast (Fig. 1) had AOU of 2-2.5 mg l⁻¹ in the deep layer in 2017, i.e. in the same order that has been
815 estimated in the KSSW before (Qian et al., 2017). The total AOU in the water column there was 50-60
g m⁻² (Fig. 6h). This water is still rather well ventilated comparing to the deep layer waters that had
been impacted by upwelling or CDW induced production in the surface layer (Fig. 6g-h). Despite its
initial oxygen depletion, Kuroshio intrusion is important source of oxygen import to the study area (Zuo
et al., 2019). Without this lateral oxygen advection, hypoxia could form much faster in larger area (Zuo
et al., 2019). Kuroshio intrusion is nutrient rich (Zhang et al., 2007b; Zhou et al., 2019) and its
820 upwelling or vertical mixing could intensify sequence of primary production in the surface,
consequently organic matter sinking producing oxygen consumption in the near-bottom layers.."

Specific comments:

Line170: how to define weak or strong stratification based on density difference here?

825

Reply: we do not define it, just comparing different regions.

Action: We changed "relatively weak" to "weaker" to avoid confusion.

830 Line239: U is the river velocity. How is U calculated?

Reply: It was calculated as discharge divided by cross-sectional area in the river mouth (which is a bit subjective, depending on exact location). However, we realized during revision that the calculation and topic is not necessary to mention in results, as there are more sophisticated studies already available, where estimates can be taken.

835 Action: We now have about this topic section only in discussion: “The faith of the river plume can be separated to the regions and processes: circulating bulge near the mouth and downstream current along the coast (Fong and Geyer, 2002; Horner-Devine, 2009). The question is how much of riverine water remains in the river plume bulge and how much is advected to the neighboring areas. It has been estimated that about 80-90% of the discharge accounts to freshwater transport of coastal current (Li and Rong, 2012; Wu et al., 2013). “

840

Track changes in manuscript

Wind-driven stratification patterns and dissolved oxygen depletion in the area off the Changjiang (Yangtze) Estuary

Taavi Liblik^{1,2}, Yijing Wu¹, Daidu Fan^{1,3,*}, Dinghui Shang¹

¹ State Key Laboratory of Marine Geology, Tongji University, Shanghai, 200092, China

² Department of Marine Systems, Tallinn University of Technology, Tallinn, 12618, Estonia

³ Laboratory of Marine Geology, Qingdao National Laboratory for Marine Science and Technology, 387P+WW Shinan, Qingdao, Shandong, China

Correspondence to: Daidu Fan (ddfan@tongji.edu.cn)

Abstract. The area off the Changjiang Estuary is under strong impact of fresh water and anthropogenic nutrient load from the Changjiang River. The seasonal hypoxia in the area has variable location and range, but the decadal trend reveals expansion and intensification of the dissolved oxygen (DO) depletion.

Two oceanographic cruises, conducted in summers 2015 and 2017, were complemented by river discharge, circulation simulation, and remotely sensed wind, salinity and sea level anomaly data. Two distinct situations of stratification and DO distributions in summers 2015 and 2017 can be explained by wind forcing and concurrent features in surface and deep layer circulation, upwelling and downwelling events.

Enhanced primary production in the upper layer in the Changjiang Diluted Water (CDW) or in the upwelled water determined the location and extent of oxygen depletion. However, pycnocline created by Kuroshio subsurface water intrusion was essential precondition for hypoxia formation. Spreading of the CDW, occurrence of upwelling and intrusion of deep layer water are strongly influenced by wind forcing.

Intensification of Chinese Coastal Current (CCC) and CDW spreading to south together with coastal downwelling caused by northerly wind were observed in 2015. This physical forcing lead to well ventilated area in north and hypoxic area of 1.3×10^4 km² in the southern part. Alteration of CCC due to Ekman surface flow and reversing the geostrophic current related to upwelling induced by summer monsoon (southerly winds) were observed in 2017. Wind-driven offshore advection in the surface layer caused intrusion of Kuroshio intrusion-derived water to shallow (<10 m depth) areas at coastal slope. Intense hypoxia (DO down to 0.6 mg l⁻¹) starting from 4-8 m depth connected to CDW and deep water intrusion in north, and coastal hypoxia linked to upwelling were observed in 2017.

Variability in wind forcing and river run-off and related changes in physical environment considerably shape extent and location of hypoxia in synoptic, seasonal and inter-annual time-scale off the Changjiang Estuary.

, revealed very different stratification and DO conditions in the area. Strongly inclined oxycline well correlated with the thermocline in both years. Southerly wind caused reversal of the Chinese Coastal Current and as a result, spreading of the CDW (Changjiang Diluted Water) caused pronounced hypoxic zone in the area east and northeast of the river mouth in 2017. Hypoxic layer started right below the CDW layer at 5-8 m depth and extended down to bottom. Strong DO depletion was also observed in the shallow coastal slope in the southern part of the study

Formatted: Font: (Default) Times New Roman

Formatted: Not Highlight

Formatted: Superscript

area. High DO utilization there closely coincided with the interaction zone of the upwelling and fresher surface water. The stratification and hypoxia pattern observed in the area in 2017 is prevailing phenomena during summers if considering the long-term wind statistics.

Northeasterly winds supported southward transport of the CDW before the survey in 2015. Consequently, low DO was found in the southern part of the study area while subsurface layer in the northern part was ventilated. Weaker than long-term average summer monsoon is required for the existence of such pattern.

Importance of the wind forcing was confirmed by remotely sensed sea surface salinity fields and by circulation simulation. We suggest wind forcing, together with river run-off are likely main contributors of determining the synoptic, seasonal and inter-annual time-scale variations of the extent and location of low DO areas off the Changjiang Estuary.

1 Introduction

Dead zones in the coastal ocean have spread since the 1960s (Diaz and Rosenberg, 2008). Besides eutrophication (Diaz and Rosenberg, 2008), climate change (Altieri and Gedan, 2015) intensifies dissolved oxygen (DO) depletion. Estuaries and other regions of fresh water influence are typically very productive regions and often experience hypoxia (Conley et al., 2009; Cui et al., 2019; Obenour et al., 2013; Testa and Kemp, 2014). Natural and anthropogenic nutrient load in these areas leads to intensive sedimentation of organic matter. DO is used by concurrent decomposition of detritus by bacteria in the sub-surface layer. Deep layers below the euphotic zone can receive DO by physical processes only – lateral advection and vertical mixing. If the decline of DO exceeds DO import or production, the DO concentrations decrease. ~~Deep layers below euphotic zone can receive DO by physical processes only – lateral advection and vertical mixing.~~

Hypoxia is a natural phenomena off the Changjiang Estuary, as evidences of its existence extend back to 2600 years at least (Ren et al., 2019). However, hypoxic area has been expanded in recent decades (Chen et al., 2017; Ning et al., 2011; Zhu et al., 2011), which can be mostly related to ~~the~~ eutrophication (Wang et al., 2016). A low DO zone off the estuary can be found from spring (Zuo et al., 2019) until decay of stratification in autumn (Wang et al., 2012). The formation and maintenance of seasonal hypoxia has been related to various physical, biogeochemical and biological processes (Ning et al., 2011). Hypoxia off the Changjiang Estuary is in literature

920 often divided to the southern and northern areas (Wei et al., 2017a; Zhu et al., 2011). The northern part features shallow (20 – 40 m) and flat sea bottom while the southern part is characterized by a deep trough with water depth > 60 m and a steep slope. Numerous small peninsulas and islands occupy in the southern part with irregular coastline.

The area is intensely impacted by huge river discharge from the Changjiang (Beardsley et al., 1985; Xu et al., 925 2018). Correlation between the CDW plume area and river discharge has been suggested by Kang et al. (2013). Nutrient rich freshwater mixes with ocean water to form the Changjiang Diluted Water (CDW). Enhanced primary production in the CDW causes intense detritus accumulation and DO consumption in the near-bottom layers (Chen et al., 2017; Li et al., 2018b; Wang et al., 2017, 2016; Zhou et al., 2019). The CDW is separated from the deeper water with a shallow halocline, which often coincides with the seasonal thermocline (Zhu et al., 2016). The shallow 930 pycnocline impedes vertical mixing and vertical DO transport downwards. Thus, the presence of the CDW provides favorable conditions for hypoxia formation in the layer below the pycnocline. Moreover, the shallow pycnocline supports accelerated warming in summer (Moon et al., 2019) and as consequence the pycnocline strengthens even more. Therefore, the spreading of the CDW strongly determines oxygen consumption and depletion in the near bottom layer.

935 Shallower areas near the river mouth are strongly impacted by tidal forcing (Li et al., 2018). However, in the open sea the contribution of tides in the vertical mixing budget is low comparing to the wind stirring (Ni et al., 2016). Abrupt wind mixing events can weaken stratification and considerably increase DO concentrations in the deep layer (Ni et al., 2016). However, such vertical mixing also cause nutrient flux to the upper layer (Hung et al., 2013) and as a result primary production in the upper layer and DO consumption in the deep layer is-are enhanced (Ni et 940 al., 2016).

Circulation and hydrography near the Changjiang Estuary are besides the CDW and wind mixing impacted by the 945 Chinese Coastal Current (CCC), and the Taiwan Warm Current (TWC) originates from the Taiwan Strait warm water in the surface and the shelf-intrusion water of Kuroshio subsurface water (KSSW) in the bottom the Taiwan Warm Current (TWC) and its northward extension, Chinese Coastal Current (CCC), and Kuroshio intrusions (Lie and Cho, 2002, 2016; Liu et al., 2017; Zhang et al., 2007b; Zuo et al., 2019). Geostrophic currents in the area are modified by wind forcing, which exhibits seasonal alternation of winter and summer monsoons (Lie and Cho, 2002). Winds from north and northeast prevail during the winter monsoon and southerly winds dominate during the summer monsoon (Chu et al., 2005). Summer monsoon favors upwelling formation in the the Eastern China Sea (ECS) (Hu and Wang, 2016), including sea areas nearby the Changjiang Estuary (Xu et al., 2017; Yang et al., 950 2019). Upwelling events bring large amounts of nutrients to the surface layer (Wang and Wang, 2007), which cause increase of primary production and decrease of DO concentrations in the near-bottom layer (Chen et al., 2004; Zhou et al., 2019). Moreover, coupling of the CDW plume and KSSW upwelling has a cumulative effect on primary production and hypoxia formation in the near bottom layer (Wei et al., 2017a). CDW spreading and TWC subsurface water upwelling are both sensitive to wind forcing, which gives rise of the hypothesis: hypoxic conditions are sensitive to wind. 955

Recent modeling study (Zhang et al., 2018) has demonstrated that the CDW is very mobile and as a result location and areal extent of bottom hypoxia is variable as well. Thus, distributions of oceanographic fields mapped during an occasional research cruise could depend on simultaneous synoptic scale forcing conditions and does not necessarily represent the hydrographical physical and chemical situation in a particular summer. In order to put

Formatted: Not Highlight

Formatted: Not Highlight

960 oceanographic cruise results ~~in~~ more general context, observed ocean variables must be linked to the forcing. The role of nutrient consumption and primary production in the CDW, in the upwelled water and their interaction have been investigated. It is clear that enhanced primary production due to upwelling and in the CDW results higher oxygen consumption rates in the near bottom layers (Chen et al., 2017, 2004; Große et al., 2019; Li et al., 2018b; Wang et al., 2017, 2016; Wei et al., 2017a; Zhou et al., 2019). The focus of this work will be on the physical forcing mechanisms that create favorable conditions for the aforementioned biogeochemical and biological processes.

965 ~~The Hypothesis-hypothesis~~ of the present study is that prevailing physical factors, wind forcing and river run-off mainly determine the stratification patterns and as consequence the location and areal extent of the DO depletion off the Changjiang Estuary. This means that changes in forcing over various time scales (synoptic, inter-annual, decadal) ~~cause~~ also cause changes in the patterns (e.g., the stratification or the location of the hypoxic area). To testify this hypothesis, we (1) ~~described~~ the observed patterns (horizontal and vertical distributions) of ~~stratification~~hydrography, chlorophyll *a* and DO off the Changjiang Estuary during the two cruises in the summers of 2015 and 2017, (2) ~~explored~~ the potential link between physical variables and DO distributions, and (3) ~~investigated~~ the forcing mechanism behind observed patterns.

970

975 ~~Following a description of the measurements and the methods used, this paper presents an analysis of (1) spatial distributions of temperature, salinity, DO and derived variables, (2) temporal changes and forcing behind the observed distributions. Finally, the analysis of our results are discussed and concluded.~~

Formatted: Font: Italic

980

2 Data and Methods

We have performed two surveys in the Changjiang Estuary and the adjacent sea on board the RV ZheyukeZhehaike-1 from 27 August to 5 September in 2015 and from 24 to 29 July in 2017, respectively. CTD (Conductivity, Temperature, Depth) and DO profiles were obtained from 110 stations in 2015 and 83 stations in 2017. ~~However, we have excluded stations inside river mouth, therefore, but 65 and 49 not all the stations were included in the present study, respectively in 2015 and 2017. Layout of the stations used in the present work is shown in~~ (Fig. 1). At all stations vertical profiles of temperature, salinity and DO were recorded with the SBE 25plus Sealogger CTD with DO sensor SBE43. The DO sensor was calibrated against water sample analyses conducted by Winkler titration method. Linear regression between sensor and sample DO data for ~~the~~ 2015 and 2017 ~~was were found respectively analyzed~~: $DO = DO_{SBE} \times 0.98 - 0.09$ ($r^2 = 0.93$ $n = 191$) and $DO = DO_{SBE} \times 0.98 - 0.06$ ($r^2 = 0.99$ $n = 98$), where DO_{SBE} is the DO recorded by SBE43 sensor (Wu et al., 2019).

985

990

995 For the 2015 cruise, chlorophyll *a* (Chl *a*) concentrations were measured from water samples as follows. About 500ml surface water was filtered through 0.7 μ m (pore size) Whatman glass fiber filters at every station with pressure lower than 15Kpa to get the particles for further analysis. To avoid the influence of light during the storage, all filters after filtration were fold up and wrapped by the aluminum foil before being put in the -20 $^{\circ}$ C

freezer. The pigments in each filter were extracted by 90% acetone and measured by fluorometric analysis using the Hitachi Designs fluorescence spectrophotometer (F-2700).

Daily satellite (Aqua MODIS) derived Chl *a* data were downloaded from <https://coastwatch.pfeg.noaa.gov/>. According to data availability mean Chl *a* field from 21-22 July, i.e. 3-4 days before our survey, is presented in the paper to illustrate primary production in 2017.

Salinity data in the present work is presented in the Practical Salinity Scale (Fofonoff and Millard Jr, 1983) and density as potential density anomaly (σ_θ) to reference pressure of 0 dbar (Association for the Physical Sciences of the Sea, 2010).

8-day running average Sea Surface Salinity (SSS) with resolution of 0.25° calculated from Soil Moisture Active Passive (SMAP) mission (Meissner et al., 2018) was used for the spatial extent estimation of the CDW from 2015 to 2018. Remotely sensed salinity well agreed with the in-situ salinity measurements (Fig. 2) at the mooring station M1 (Fig. 1).

Reprocessed 6 hourly wind observations with horizontal grid size resolution of 0.25° from 1993 to 2018 downloaded from Copernicus Marine Service (product ID WIND_GLO_WIND_L4_REP_OBSERVATIONS_012_006) was used to describe wind conditions. Wind stress was calculated following Large and Pond, (1981):

$$\tau = \rho_{air} C_D U_{10}^2 \quad (1)$$

where C_D is the drag coefficient and U_{10} is the wind speed at the reference height of 10 m above sea level.

Current speed and direction from the Copernicus Marine Service reanalysis product GLORYS12V1 from 1993 to 2018 was downloaded. The global eddy resolving model has regular horizontal grid with step of approximately 8 km ($1/12^\circ$) resolution and standard vertical levels with resolution increasing from 1 m near the surface to 8 m around 50 m depth and 17 m around 100 m depth. Remotely sensed and in-situ observed temperature, salinity, and sea level were assimilated to the model. The model has too rough resolution to estimate details of meso- and finer-scale features in the area. However, it can be used to estimate the general current patterns. Simulated current field reasonably well reproduced the observed spreading direction of the CDW.

Daily mean sea level anomaly and meridional and zonal components of absolute geostrophic velocity based on satellite altimetry were downloaded from the Copernicus Marine Service (product DATASET-DUACS-REP-GLOBAL-MERGED-ALLSAT-PHY-L4). The sea level anomaly is defined as the sea surface height above the mean sea surface during reference period 1993-2012. Horizontal and temporal resolution of the dataset are 0.25° and one day, respectively.

Depending on marine organisms, hypoxia can have various definitions (Vaquer-Sunyer and Duarte, 2008). In the present study, hypoxia was defined as DO concentration of $<3.0 \text{ mg l}^{-1}$. In order to estimate oxygen consumption, the apparent DO oxygen utilization (AOU) was estimated. AOU is the difference between DO concentration at the saturation level and measured DO concentration in water with the same temperature and salinity and is calculated as follows

$$AOU = DO_s - DO_M \quad (2)$$

where DO_s is DO concentration at the saturation level (Weiss, 1970) and DO_M is the measured DO concentration.

Total AOU (g m^{-2}) in the water column was calculated as

$$AOU_{TOT} = \sum_{z=0}^{z=h} \begin{cases} 0, & \text{if } AOU \leq 0 \\ AOU(z)dz, & \text{if } AOU > 0 \end{cases} \quad (3)$$

Formatted: Font: Italic

Formatted: Font: 12 pt

Formatted: Font: (Default) Times New Roman

Formatted: Font: 12 pt

Formatted: Font: (Default) Times New Roman

Formatted: Font: 12 pt

Formatted: Font: Not Italic

Formatted: Font: Not Italic

Formatted: Font: Not Italic

Formatted: Font: Not Italic

Formatted: Font: Italic

Formatted: Font: Italic

where $AOU(z)$ is the AOU profile and h is the water column depth.

The upper boundary of the DO depletion (UBD) was defined as the AOU isoline 2 mg l^{-1} . Different authors have used various criteria to define water masses in the region. The cold bottom in the area water in the area mostly originates from the KSSW (Liu et al., 2017). Therefore we define deep layer water as the upper boundary of the Kuroshio (UBK) subsurface water mass as isotherm $24.5 \text{ }^\circ\text{C}$ (Zhang et al., 2007a).

Daily (2015 and 2017 summer) and monthly (2001-2018) river discharge data from Datong hydrological station (see location in (Xu et al., 2018)) were used in analysis.

Width of the buoyant coastal current was estimated according to (Lentz and Helfrich, 2002) as

$$W_p = (c_w/f) (1 + c_w/c_a) \quad (4)$$

$$\text{where } c_w = (g' h_p)^{1/2}; c_a = ag'/f; h_p = (2Qf/g')^{1/2}; g' = gd\rho/\rho \quad (5)$$

where f is Coriolis force, Q is the volume transport (taken as river discharge), $d\rho$ is the density difference between the plume and ambient fluids (ρ) and α is the coastal slope.

Remotely sensed salinity data are linearly interpolated from four closest grid points to the location of measurements.

3 Results

3.1. Spatial patterns of hydrography, Chl a and oxygen

In order to link the thermohaline structure and DO observations in the following we next analyze temperature, salinity, stratification and DO distribution patterns observed in summers 2015 and 2017. In order to illustrate primary production, subsequent organic matter degradation and oxygen consumption Chl a data is presented.

The water of $SSS < 30\text{-psu}$ was observed along the coastal zone of the entire study area in 2015 (Fig. 3a). The 25 isohaline 25-psu reached to 29.3° N in the southern part of the study area while its northern boundary was at 31.7° N near the mouth of the Changjiang Estuary in 2015. In 2017 the 25 isohaline 25-psu reached only to 30.6° N in the southern part of the study area (Fig. 3b). While fresher water than 25-psu was also observed in the east and northeast off the Changjiang Estuary. Thus, the CDW southward spreading has been prevailing before the survey in 2015, but the CDW eastern and northeastern diversion was observed prior to survey in 2017.

The surface temperature (SST) was generally lower in the study area in 2015 (Fig. 3c). The maximum SST in the study area was $28.3 \text{ }^\circ\text{C}$ ($31.3 \text{ }^\circ\text{C}$) in 2015 (2017). Colder surface water was observed near Zhoushan Islands and along Zhejiang the coast between (28.5° N to and 31° N), and in the northern part of the study area ($>31.5^\circ \text{ N}$) in both years (Fig. 3c-d). The SST was much lower in these regions, but colder area covered smaller areas in 2017 (Fig. 3d) comparing to 2015.

The near-bottom temperature difference between the two surveys was particularly large in the northern part of the study area (Figs. 3-5g-h, 4a, 5a). Near-bottom temperature was $24\text{-}25 \text{ }^\circ\text{C}$ at $20\text{-}30 \text{ m}$ sea depth in 2015 (Fig. 4a) while it was $21\text{-}22 \text{ }^\circ\text{C}$ in 2017 (Fig. 5a). Likewise, near-bottom water was saltier in 2017 (Figs. 3e-f, 4d, 5d). The

Formatted: Font: Not Italic

Formatted: Font: Italic

Formatted: Font: Italic

Formatted: Font: Italic, Subscript

Formatted: Font: Italic

Formatted: Font: Italic, Subscript

Formatted: Font: Italic

Formatted: Font: Italic, Not Superscript/ Subscript

Formatted: Font: Italic

Formatted: Font: Italic, Subscript

Formatted: Font: Italic

Formatted: Font: Italic

Formatted: Font: Italic

Formatted: Font: Italic

location of minimum near-bottom temperature was at 50-60 m sea depth in the southern and central part of the study area in 2015 (Fig. 3g and Fig. 4b-c). The minimum temperature zone was closer to the coast and at shallower depths in 2017 (Fig. 3h and Fig. 5a-c).

Spatial patterns of Changes of stratification in the study area are described by the difference between the surface and near-bottom layer density (Fig. 6a-b). Relatively weaker stratification ($< 3 \text{ kg m}^{-3}$) was observed in the northern part of the study area in 2015 (Fig. 6a). KSSW was present only at the offshore part in north (Figs. 4a,d). Stratification was stronger ($>3 \text{ kg m}^{-3}$) in the area south off the Changjiang Estuary, being particularly strong ($>6 \text{ kg m}^{-3}$) at-in areas of 20-30 m sea-bottom depth (Fig. 6a). In this area, the CDW covered the surface layer (Figs. 4e-f), and cold and saltier water mass occupied the near-bottom layer (Fig. 4b-c, e-f). Near the coast and offshore such strong stratification was not observed (Fig. 6a), i.e., the dense deep layer water did not intrude into the shallower areas and the CDW did not spread further offshore (Fig. 4a-c and Fig. 3 a.c.e.g). The UBK had considerable inclination from 24 m depth near the coast to 48 m depth at 80-85 km distance across shore in the southern section in 2015 (Figs. 4c.f and 7c). Opposite inclination, i.e. downwelling, was observed in the central station in 2015 (Fig. 4b.e). The boundary was at 38 m depth at the base of coastal slope, but at 17 m depth further offshore (Figs. 4b.e). Downwelling had pressed the salinity 30 isoline down to 40 m depth in the central section in 2015 (Fig. 4e). Probably onshore advection of more saline offshore water was pushed over fresher coastal water and caused vertical mixing.

Strongest stratification ($>6 \text{ kg m}^{-3}$) was observed in the northern part of the study area in 2017 (Fig. 6b). The cold UBK was located at depths of 4-8 m in most of the northern section (Figs. 5a, 7d). Above the strong pycnocline was warm and fresh water, the CDW (Fig. 5a,d). The areal extent of very strongly stratified ($>6 \text{ kg m}^{-3}$)-region fitted with the area of CDW distribution in the surface layer (Fig. 3b). Stratification was weaker ($<3 \text{ kg m}^{-3}$) in the very shallow areas ($< 10 \text{ m}$, Fig. 6b), where cold and saltier water mass did not exist, and in the southeastern part of the study area, where the CDW did not spread and bottom water was warmer than at the core of the cold water mass (Figs. 3f,h and 5a-f). Stratification pattern in the central and southern section was characterized by strong inclination of the isopycnals. The UBK was at 50 m depth at 110 km distance (from the western end of the section) offshore and at 7-8 m near the coast (0 km distance) in the southern section (Fig. 5c,f). Surfaced UBK, i.e. upwelling was observed at 70-80 km distance in the central section (Fig. 5b). Warmer and fresher surface water were observed both shoreward and offshore side from the upwelling core (Fig. 5b, e). Thus, coupling of the riverine fresher water and upwelling could be expected there.

Low DO concentrations ($2-3 \text{ mg l}^{-1}$) in the near-bottom layer occurred at sea depths in areas of 25-60 m bottom depth in the southern and central part of the study area in 2015, affected an area of $1.3 \times 10^4 \text{ km}^2$ approximately (Figs. 4h-i, 6e). Higher Chl *a* values along the coastline in the central and southern part illustrate the role of primary production in the CDW and subsequent processes resulting oxygen consumption in the deeper layers (Fig. 6c). Although due to downwelling the low DO water mass is pressed deeper and further offshore while CDW is pushconstrained closer to the coast (Figs. 4e h). Higher Chl *a* value in one station in the northern part (at 31.6° N and 122.6° E) coincided with the lower (<30) surface salinity intrusion (Fig. 6a). Elevated Chl *a* values further offshore (around 31.5° N and $123.2-123.5^\circ \text{ E}$) did not coincide with the CDW (Figs. 3b, 6c). UBD and UBK were strongly linked in the southern and central section in 2015 (Figs. 4j-k, 7a,c). However, the boundaries coincided only in the offshore side at the northern section (Fig. 4j). This was the only section shown in Figs. 4-5, where the UBK and U \O BD did not coincide (Fig. 4j). Likewise, this region differs from the rest (except shallower areas with

Formatted: Font: Italic

sea depth <20 m) of the observations by high near bottom DO values (Figs. 4g, 6e). The across-shore lateral distribution of DO, AOU and temperature under the thermocline reveal the linked structure in the northern section in 2015 (Figs. 4a,g,i). The coldest and lowest DO water is located in the offshore side of the section. Around 40-50 km distance, there is lateral maximum of the DO and temperature. Slightly lower DO and temperature were observed at 10-30 km. Similar lateral alternation from higher to lower and back to higher Chl *a* (Fig. 3c) and in opposite phase in the surface temperature and surface AOU (lower-higher-lower, Fig. 4a,g), respectively, can be found in the northern section in 2015 (Fig. 3c). We discuss about possible reasons of such distributions in next subchapter. Near-bottom DO concentrations further offshore (east) and in the north were 3-5 mg l⁻¹ and higher in shallower depths in 2015 (Figs. 6e, 4g-i). Low DO area (2-3 mg l⁻¹) only partly overlapped with the CDW distribution, but fitted well with the area occupied by cold (< 20 °C) water mass in the near-bottom layer (Figs. 4a-c, 4g-l). The vertically integrated AOU maximum (>150 g m²) pattern was observed between 30-31° N and 123-124° E in 2015 (Fig. 6g). Latter area did not coincide with the Chl *a* distributions. In fact very low Chl *a* values were observed at 30.5-31° N and 123-124° E (Fig. 6c) while oxygen depletion (the total AOU) was there rather high (Fig. 6e). Latter indicates that oxygen depletion in the southern and central part has developed over longer periods.

Two low DO concentration (<3 mg l⁻¹) zones were observed in the near-bottom layer in 2017 (Figs. 5g-i and 6f). The one in the north well overlapped with the low salinity CDW and strong stratification area (Fig. 6b, 6f). Hypoxia there started at 45-8 m depth already and was closely linked to the location of the pycnocline (Figs. 5a, 5d, 5g). Lowest DO and highest AOU of all our measurements were observed in the northern part in 2017 (Figs. 5g,j). Some profiles showed DO nearly 0.6 mg l⁻¹ conditions and AOU over 6 mg l⁻¹. High Chl *a* were observed in the northern part, displaying the intense production in the upper layer (Fig. 6d). The second low DO concentration zone was observed in shallow depths (10 - 30 m) at the coastal slope in the southern and central part of the study area and overlapped with colder SST and lower SSS lower SST and SSS upwelling region (Figs. 5b-c, e-f, h-i). This indicates that interaction-coupling between coastal upwelling, which bring subsurface water to shallower depths (euphotic zone) and fresher riverine surface water, created favorable conditions for the primary production in the upper layer and concurrent DO consumption and depletion in the deep layer (Figs. 5h,i,k,l). Higher Chl *a* concentrations in the upwelling areas revealed from the satellite image, although not as high as in north (Fig. 6d). The vertically integrated AOU had highest values (>150 g m²) in the northern part of the study area in 2017 (Fig. 6h).

The low-high DO concentration AOU zones in the near-bottom layer can be found in various regions sea of different depths, e.g., as shallow as 4-4 m in 2017 (Figs. 4j-l, 5j-l). Strong and shallow enough stratification makes DO depletion possible in such a shallow depth. The question is whether the DO depletion is linked to a certain physical property of water, e.g. to a temperature-, salinity- or density- isoline of water. We determined the AOU isoline 2 mg l⁻¹ as the upper boundary of the DO depletion, i.e. the oxycline. We found high correlation ($r^2 = 0.81$, $p < 10^{-10}$, $n = 44$ in 2015, and $r^2 = 0.98$, $p < 10^{-10}$, $n = 34$ in 2017) between isotherm 24.5 °C_{UBK} and AOU-UBD isoline 2 mg l⁻¹-depth. Thus, the vertical location of the UBK thermocline determines the vertical location of the oxycline-UBD largely. The cold KSSW is denser than water above and the resulting thermocline/pycnocline provides barrier for vertical mixing and under the eline below DO depletion can develop. There was an inclination of the both clines in both years (Fig. 7). The inclination was particularly steep in 2017. Both isolines were located around >50 m depth in the southeastern corner of the study area while in the shallow areas in the west and north

Formatted: Font: Italic

Formatted: Estonian

Formatted: Superscript

Formatted: Superscript

the same layer was at 45 – 840 m depth (Figs. 7b,d). Such an inclination of isotherms and cold SST near the coast is an indicator of upwelling. Deeper colder water intruded along the coastal slope shallower to replace the former upper layer water. The inclination of clines was not that pronounced and it was rather north-south directed in 2015 (Figs 7a,c). Lower correlation in 2015 is caused by discrepancy of the two isolines in the northern part in 2015.

1160 This indicates some other processes than Kuroshio water intrusion, e.g. vertical mixing, vertical movement of pycnoclines or advection altered subsurface conditions there.

-It is noteworthy that the high vertically integrated AOU (Fig. 6g) area overlapped with shallow position of isolines in 2015 (Figs. 4k, 7a, 7c.). It means that high total AOU there (comparing to neighboring areas) was related both to the thick subsurface DO depleted layer and not to the lower-higher (comparing to surrounding area) DO concentrations AOU.

1165 We have captured two completely distinct situations of stratification and DO distributions in summers 2015 and 2017. The differences between the two years are outlined-summarized in the Table 1. Prevailing of either pattern in the physical fields has consequences to the biogeochemical fields and ecosystem in general in the area. The main questions addressed next are: what are the main drivers causing the distinct patterns? What is the quantified 1170 forcing behind formation of the patterns?

1175

1180 **3.2. Forcing, time-series**

The observed discrepancies of general features in the two cruise surveys can be driven by several forcing mechanisms. The riverine water is a source of buoyancy flux, causing current to flow south along the coast. Mean discharge at Datong hydrological station in the two summers (1 June to 31 August) was rather similar, 44 000 - 45 000 m³s⁻¹. We consider the time lag of 1 week for water propagation from Datong to the river mouth (Li and Chen, 2019) in further discussion.

1185 Comparing two years discharge data in June, discharge was higher in 2015. Contrary in July discharge was higher in 2017. Daily discharge maxima peaked at 58 000 m³s⁻¹ on 1 July in 2015 and at 70 000 m³s⁻¹ on 13 July in 2017. 1190 According to the typical residual current velocities off the estuary (Peng et al., 2017) and along the coastline in the south (Wu et al., 2013), it should take a few days to weeks for the water from the river mouth to reach offshore as we registered in 2017 or to Zhejiang-the southern part coast in the south in-in 2015. We assume that 7 days accumulated run-off (or wind forcing) is enough to alter the field distributions off the estuary. Mean river flow during thea week before surveys was 30 000 m³s⁻¹ in 2015 and 65 000 m³s⁻¹ in 2017, respectively. The question

1195 is how much of riverine water remains in the river plume bulge and how much is advected to the neighboring areas. The discharge Rossby number $R_d = U/Bf$ (Fong and Geyer, 2002), where U is the river inflow velocity, B is the river mouth width (34 km) and f is the Coriolis parameter ($7.5 \cdot 10^{-5}$), describes the share of riverine water in the bulge and downstream current. The estimated R_d varied between 0.08 and 0.22 in 2015 and 2017. Relatively low R_d shows that most of the riverine water contributes to the coastal geostrophic current but less to the bulge.

1200 Variations in discharge influence the across-shore extent of plume and the width of the buoyant current. According to the theory by Lentz and Helfrich (2002) the width W_p of buoyant current would be 770 km in the case of ambient and CDW water density difference of 10 kg m^{-3} , coastal slope of 10^{-4} and discharge of $65\,000 \text{ m}^3 \text{ s}^{-1}$ before our survey in 2017. The width would be 48–55 km if the inflow volume of $30\,000 \text{ m}^3 \text{ s}^{-1}$ in 2015 was considered. Thus, the variability in the river discharge only somewhat explain the discrepancy between the two

1205 surveys, particularly more extensive spreading of the CDW eastward in 2017. However, it does not explain the northeast advection of the CDW that far in 2017. Likewise, it remains unclear why southward transport of the CDW was much more limited in 2017 than 2015. While several indicators hint that wind-driven transport could be behind the discrepancy between the 2015 and 2017 observations, including stronger across shore inclination of the pycnocline, offshore advection of the CDW, and onshore advection of the colder sub-pycnocline water in 2017.

1210 Such features were not found during the survey in 2015, but southward advection of the CDW revealed instead. Since our surveys are conducted annually one month apart, the differences between the two surveys might be associated with the annual cycle in wind climate. Our hypothesis is that the dominant factor behind the discrepancy of the two surveys is wind forcing and possibly its annual cycle.

As argued previously, we assume the thermohaline fields in the study area were established by the forcing one week before. Mean wind, sea level anomaly, surface currents and bottom currents during one week prior to the surveys are presented in Fig. 8. The mean airflow wind direction was from northeast prior to the 2015 survey (Fig. 8a) and from south prior to the 2017 survey (Fig. 8b). Northeasterly wind should cause downwelling and accelerate alongshore buoyant current towards the south. This current was clearly detectable-visible in the mean surface current plot in 2015 (Fig. 8c), along the coast from 32.5° N to 28° N . Such coastal current did not reveal before the 2017 survey (Fig. 8d). Weak mean flow towards the east or northeast could be noted near the mouth of the Changjiang River in 2017 (Fig. 8d). Likely, the buoyant coastal current was altered and the CDW was transported across shore by southerly wind forcing. Thus, simulated current patterns and wind forcing prior to the two surveys were qualitatively in accordance with observed salinity fields in the surface layer (Figs. 3a-b). Main difference between the two years in the bottom layer was the stronger northward flow in 2017 (Figs. 8e-f).

1225 Penetration of the deep layer water to the shallower areas, towards the river mouth occurred in 2017 (Fig. 8f). This coincided with our observations in terms of the stronger inclination of clines (Figs. 7b,d) and presence of the colder KSSW water mass in the northern part of the study area in 2017 (Fig. 3h). Because southerly wind forced offshore transport of the surface water, deep layer water intruded to the shallower depths for compensation in 2017. It has to be noted that southward coastal flow was almost negligible (unlike in the surface) in the bottom layer in 2015, showing the baroclinic nature of the current.

1230 This suggested pattern of processes based on field surveys and modelling data can be confirmed by mean sea level anomaly during the surveys (Figs. 8g,h). There is strong sea level gradient between near-shore and offshore in both years. Higher sea level can be found along the coast from the northern boundary of study area to 30° N in south in 2015 and as a result, geostrophic current is southward. This is combined effect of the lighter riverine water and convergence of the shoreward transported upper layer

Formatted: Font: Italic

1235 water. This is in accordance with our observation of the downwelling in the central section (Figs. 4b,e,h,k) while
such a phenomena did not reveal in the southern section (Figs. 4c,f,i,l) in 2015. Downwelling occurred
1240 simultaneously with along-shore southward current in the northern part according to the sea level anomaly (Fig.
8g) and modelled current field (Fig. a,c). This could explain the well ventilated and warmer near-bottom waters in
north in 2015 (Fig. 4a,g,j). Opposite gradient, i.e. lower sea level anomaly near coastline were observed in 2017.
This is a typical sign of divergence, i.e. offshore transport of the surface water and consequent upwelling along
the coastline. The zonal pattern of sea level from the river mouth to offshore (high-low-high sea level, Fig. 8h)
agrees with our observation of the upwelling in the central section (Figs. 5b,e). As a result of sea level anomalies,
geostrophic current towards north at 28.5-31° N and to offshore near the river mouth were observed in 2017.

In order to verify the sensitivity of the buoyant coastal current to wind forcing, simulated current and wind data
1245 from June to September in 1993–2018 were used. First, we calculated daily mean meridional (alongshore) upper
layer (0-5 m) current velocity component v_m at the zonal section of 31° N (section S1) from 122.1° to 122.6° E
(see red-dashed line in Figs. 8c-d). Correlation was calculated between the current velocity component v_m and
wind (see the location in Fig. 1) from different directions (full circle by 10° steps). The best correlation ($r^2 = 0.76$,
 $p < 10^{-10}$, $n = 3025$) was found with the one-day (prior to the modeled current value) mean SE–NW wind velocity
1250 component w_c (Fig. 9). Thus, the meridional current along the coast well correlates with wind.

Simulated near-bottom currents (Fig. 8f) suggest that cold and saltier water (comparing to 2015 observation) was
adverted to the northern part of the study area as compensation flow to the near-surface offshore flow in 2017.
Moderate winds before the 2017 survey (Fig. 10a) could not mix the cold and DO depleted deep layer water into
the upper layer. However, stronger wind impulse with speeds up to 11-12 m s⁻¹ occurred a few days before the
1255 start of the survey in 2015 (Fig. 10a). Upper mixed layer depth created by wind stirring was estimated by the
formula describing the turbulent Ekman boundary layer $h = 0.1 u_* / f$ (Csanady, 1981), where $u_* = (\tau / \rho_w)^{1/2}$ is
friction velocity, ρ_w is water density, τ is wind stress and f is Coriolis parameter. Vertical mixing reached down
to 15-16 m depth according to this empirical method before the 2015 survey. Note that our estimation is based on
6-h average wind speed and stronger winds, which probably cause deeper mixing to occur in on shorter time scales
1260 probably causing deeper mixing. Thus, wind stirring could considerably weaken the stratification before the 2015
survey, as evident by the presence of warmer, fresher water with higher DO concentration in the deep layer.

However, also advection from north (Fig. 8c) and downwelling (Fig. 8g) likely contributed to the weakening of
stratification and ventilation of the northern part in 2015. Water from north is colder and causes convective mixing
and weakening of the thermocline. The effect of downwelling can be well seen in the central section (Fig. 4b,e,h,k).
1265 Sea bottom is more flat in the northern part and therefore the sub-thermocline distributions in the case of
downwelling showed up there as lateral gradients (Figs. 4a,d,g,j). Closer look to satellite derived daily sea surface
temperature (Donlon et al., 2012) and sea level anomaly maps indicate that northern section in 2015 could have
been impacted by cold mesoscale cyclonic eddy origin from north. Effect of an cyclonic eddy can be probably
seen in Figs. 4a,j. There is lower temperature at distance of 50-60 km with uplifted AOU isolines. Upward lifted
1270 isopycnals and oxygen isolines are typical features of cyclonic eddies (Czeschel et al., 2018). We do not investigate
further the exact contribution of each process, since it is not under the scope of the present work. However, it is
clear, that all the processes evoke by northerly wind and cause weakening of stratification and vanishing of the
colder water mass, which is essential for the hypoxia formation according to our observations in all other sections.

Since the wind was from the northeast before the survey (Fig. 8), downwelling can be responsible for this weaker stratification as well.

Further we analyzed time-series of wind speed (Fig. 10a), SE-NW wind stress component (τ_c , Fig. 10b), meridional current velocity component (v_m , Fig. 10c) at the section S1, and the Changjiang river run-off (Fig. 10d) in June-September 2015 and 2017 (Fig. 10). Wind stress $\tau_c > 0$ and northward current component prevailed from June to early August in 2017 (Fig. 10b). Larger wind stress events alternated with calmer periods from June to late August in 2015. During the periods of low $\tau_c > 0$, current was often directed southward. The $v_m < 0$ occurred more frequently in June-July 2015 compared to the same period in 2017 (Fig. 10c). Latter is reflected in monthly salinity distributions (Fig. 3a-b). We defined the CDW as salinity of < 30 psu and calculated its spatial monthly occurrence from June to September in 2015-2018 using satellite surface salinity distributions (Fig. 11). Lowest areal extent of the CDW was observed in September in both years, 2015 and 2017. The CDW mainly advected to the northeast and east in all summer months in 2017. Northeastward transport of the CDW could be noted also in 2015, but the CDW occupied areas in the southern part of the study area as well. Thus, the satellite derived salinity confirms our in-situ observations of southward flowing of the CDW. We can conclude that our survey in 2017 well described the prevailing situation of the CDW spreading in summer 2017. In summer 2015, we captured the situation, where the CDW spread to the south, but during summer northeastward spreading occurred as well. The CDW spreading in 2016 and 2018 was rather northeastward (similar to 2017). It is noteworthy that coverage of the CDW was clearly larger in 2016 than we observed in 2017 while it was more limited in 2018. The CDW spreading presented in Fig. 11 is further analyzed in relation to inter-annual wind and river forcing, and in the context to previous studies in the discussion.

Next we make an attempt to quantify the two CDW spreading cases caused by wind forcing through analyzing meridional currents v_m at section S1 (see Fig. 8c-d) and wind data from the period June-September in 1993-2018. We grouped averaged the simulated v_m to different the wind velocity w_c classes component classes with step of 0.25 ms^{-1} and took average of the each group. By doing this, we found relation between mean w_c and v_m . We found that if the daily mean wind velocity component $w_c = 0 \text{ m s}^{-1}$, current velocity component v_m would be on average -13 cm s^{-1} (i.e., southward) at S1. We can assume that this is the mean geostrophic component of the current velocity. Daily mean wind velocity component w_c of 5.6 m s^{-1} is required to reverse the current and have the same magnitude at S1 ($v_m = +13 \text{ cm s}^{-1}$). This corresponds roughly to the wind stress τ_c of 0.04 N m^{-2} . Wind stress τ_c of 0.02 N m^{-2} corresponds to the v_m of 0 cm s^{-1} , i.e., coastal current is altered. There are two main wind-driven processes that contribute to the alteration of the coastal current. First is the direct effect of wind stress and resulting Ekman surface current. Secondly, southerly winds cause divergence and upwelling at the coast and alter sea level distributions. When upwelling is evoked, alongshore geostrophic current, resulting from the cross-shore gradient between colder-denser and warmer-lighter offshore water, is rather to north. The mean sea level anomalies during our surveys in 2015 and 2017 illustrate well this phenomenon (Fig. 8g-h). The joint effect of the two processes explain relatively low wind stress required for the alteration of the circulation regime.

We analyzed the simulated current data in June-September from 1993 to 2018 and averaged the cases, when daily mean wind stress component τ_c was < 0 and $\geq 0.02 \text{ N m}^{-2}$ (Fig. 12). The same circulation features, but more pronounced, stand out as before the surveys in 2015 and 2017 (Fig. 8). In the case of $\tau_c < 0 \text{ N m}^{-2}$ southerly flow prevailed in the surface layer along the coast (Fig. 12b) and the mean currents in the near-bottom layer were rather

Formatted: Font: Not Italic

Formatted: Font: Italic

Formatted: Font: Italic, Subscript

Formatted: Font: Italic

Formatted: Font: Italic, Subscript

Formatted: Font: Not Italic, Not Superscript/ Subscript

1315 weak (Fig. 12d) as before our survey in 2015 (Figs. 8c,e). In the case of $\tau_c \geq 0.02 \text{ N m}^{-2}$ surface flow was northward along the coast, to northeast near river mouth (Fig. 12a) while, and shifted north or towards the river mouth in the deep layer (Fig. 12c) as before our survey in 2017 (Fig. 8d,f). Thus, latter supports our hypothesis of the wind-induced simulated current patterns in 2015/2017 (Fig. 8a-f).

1320 Discussion

1325 The main reason for the oxygen consumption and concurrent hypoxia is decomposition of organic matter by bacteria in the sub-surface layer. There is a strong link between primary production in the upper layer and oxygen consumption in the near bottom layer (Chen et al., 2017, 2004; Wang et al., 2017, 2016; Wei et al., 2017a; Zhou et al., 2019). The processes accompanied with enhanced primary production, spreading of the riverine nutrient rich CDW and FWCKSSW upwelling, are dependent on wind and river forcing. The effects of wind and river discharge on the spatiotemporal variability of stratification and oxygen depletion will be discussed next.

1330 Two distinct stratification, Chl *a* and DO distribution patterns were observed in the area off the Changjiang Estuary in the summers of 2015 and 2017. There was a stronger DO depletion in the southern part of the study area, off Zhejiang coast in August-September 2015, while intense hypoxia was observed in the northern part of the study area in July 2017. Likewise, remarkable DO depletion was observed in the southern part at-in the upwelling zone region in 2017. Similar hypoxia patterns in August (our July 2017 observations) and October (our August-September 2015 observations) were observed in 2006 (Zhu et al., 2011). As we have argued, the main reasons for the different spatial hypoxia patterns are variations in the wind forcing and river discharge. Summer monsoon and higher discharge both favor across-shore transport of CDW and development of hypoxia in the northern part of the study area. Both, maximum frequency of southerly wind and river discharge in the annual cycle occur in 1340 July-August (Figs. 13a,c). Thus, our observations conducted in late August - early September 2015 and late July 2017 illustrate the annual cycle of forcing and latter reflect in oxygen and stratification patterns. On the other hand summer monsoon and river discharge wasere close to average in the whole summer of 2017 while the summer monsoon was clearly weaker in 2015 (Fig. 13a-b). Thus, our observations reflect also the differences in forcing and concurrently the DO distributions between two summers, i.e. inter-annual difference. In accordance with the 1345 annual cycle of wind (Fig. 13a), highest frequency of upwelling events occurred in July-August as well (Xu et al., 2017). Wang et al. (2012) explained the annual cycle of the location of near-bottom DO minimum by seasonal change of stratification due to river discharge and warming/cooling of the upper layer. We suggest that the southern location of the DO minimum in June and September, and the northern location, as observed in July-August 2006 (Fig. 3 in Wang et al. (2012) paper), are related also to the seasonality of wind forcing, and respective 1350 transport surface current and compensating KSSW intrusion in the deep layer.

In figure 11, we presented monthly occurrence of CDW (as salinity < 30) from June to September 2015-2018. It is clear from fig. 11 that CDW transport offshore (to northeast) has occurred in all years, including 2015. However, One-one can see how year 2015 distinguishes differs with low value in the inter-annual time-series of wind stress of $\tau_c \geq 0.02 \text{ N m}^{-2}$ (Fig. 13a-b) and with considerable southward advection of the CDW (Fig. 11). Monthly mappings of bottom oxygen in 2015 (Li et al., 2018b) does not show significant oxygen depletion in north in any month while deteriorated hypoxia (comparing to our observations) in south occurred in October. This well demonstrates that wind regime plays an important role in the inter-annual variations of the hypoxic area location (Fig. 6e-f). Year 2016 stands out in terms of wind forcing close to inter-annual mean (Fig. 13b), but with very high river discharge (Fig. 13d). One can see that offshore advection prevailed in 2016 (Fig. 11). This indicates that if wind forcing is close to long-term average hypoxia more likely will occur rather in the east of the river mouth (northern part of study area) and hypoxia occurrence in the south is more limited. This can be confirmed by our observations in 2017. River discharge and $\tau_c \geq 0.02 \text{ N m}^{-2}$ occurrence were both similar to long term mean in 2017 (Fig. 13) and we observed hypoxia and CDW water in the northern part. In other words It means, hypoxia in the southern part (as we observed in 2015) occurs if the summer monsoon is considerably weaker than long-term mean. Indeed, hypoxia in the south has been quite rare in 1998 – 2013 (Chen et al., 2017). As a consequence of large river runoff, clearly largest CDW spreading area occurred in year 2016 out of the four years (Fig. 11). Occurrence of wind stress $\tau_c \geq 0.02 \text{ N m}^{-2}$ was higher than average (Fig. 13b) and river discharge was lower than average in 2018 (Fig. 13d) and this reflected well in the CDW distribution (Fig. 11). One can see that CDW covered smallest area out of four years and prevailing transport direction was towards the north or northeast (Fig. 11). Correlation between the CDW plume area and river discharge has been suggested by Kang et al. (2013). From our stratification and DO distribution observations (Figs. 3-7) and their dependence on wind forcing (Figs. 8-10, 12), and CDW spreading direction and extent (Fig. 11), DO depleted area should could have occurred in the northern part both in 2016 and 2018, with larger extent than in the former year. Hypoxia in the northern part in 2016 has been reported (Zhang et al., 2019). Lower than average river discharge and close to average occurrence of $\tau_c \geq 0.02 \text{ N m}^{-2}$ (as in 2016) occurred in 2006 (Figs. 13b,d), when hypoxia registered (Zhu et al., 2011). We estimated that wind stress of $\tau_c \geq 0.02 \text{ N m}^{-2}$ is necessary to alter the geostrophic coastal current and create favorable conditions for hypoxia in the northern part. Compared with inter-annual mean (1992–2018) in same months, the occurrence of $\tau_c \geq 0.02 \text{ N m}^{-2}$ in June – September in 2015 and 2017 was relatively lower (Fig. 13). The same applies to the comparison of the months July–August. River discharge in June – September was close to the inter-annual mean (2001–2018) in both years. Slightly lower (higher) discharge than average occurred in 2015 (2017) if only the months July–August were taken into account. Inter-annual variations of occurrence of wind stress $\tau_c \geq 0.02 \text{ N m}^{-2}$ in July–August are quite large (Fig. 13a). When the occurrence of $\tau_c \geq 0.02 \text{ N m}^{-2}$ was $\geq 50\%$ in the summers of 1995, 2012, 2013, and 2018; stratification and DO patterns could have probably occurred as coastal upwelling-related hypoxia in the south and large hypoxic area in the north as we observed in 2017 (Fig. 6b,f,h). Large hypoxic area in the north has have been documented for instance in August 2012 (Li, 2015) and August 2013 (Ye et al., 2016; Zhu et al., 2017). Contrary, in summers when the occurrence of $\tau_c \geq 0.02 \text{ N m}^{-2}$ was less than inter-annual mean (1992, 1993, 1996, 1998, 1999, 2002, 2007-2009, 2014), considerable hypoxia-oxygen depletion was also expected to have occurred in the southern part as we observed in 2015. Such situation has been captured for instance in 1998 (Wang and Wang, 2007) and in 1999 (Li et al., 2002). However, on the top of the inter-annual variability and annual cycle are synoptic scale changes of wind-driven currents and river forcing.

Formatted: Highlight

Field Code Changed

Field Code Changed

1395 which likely influence the distributions on shorter time scales (Fig. 10). Thus, when planning hypoxia related measurement campaigns in future, it is worthwhile to take into account wind-driven transport, river discharge, remotely sensed salinity and altimetry to forecast spreading of the CDW, upwelling occurrence and deep water intrusion and according to latter factors estimate potential hypoxic area location prior to field works. This could allow more efficient use of ship time and more detailed sampling of the hypoxic area.

1400 The faith of the river plume can be separated to the regions and processes: circulating bulge near the mouth and downstream current along the coast (Fong and Geyer, 2002; Horner-Devine, 2009). The question is how much of riverine water remains in the river plume bulge and how much is advected to the neighboring areas. It has been estimated. The estimated discharge Rossby number indicated that most of the river discharge contributes to the downstream geostrophic current. It well agrees with earlier estimates that about 80-90% of the discharge accounts to freshwater transport of coastal current (Li and Rong, 2012; Wu et al., 2013). This means that most of the river discharge does not remain in the river plume bulge, but impacts the surrounding areas off the estuary. Applying linear regression analysis between wind and modeled current velocity we estimated the southward geostrophic component of the current velocity to be on average 13 cm s⁻¹ at section S1. The southward coastal current was measured in winter by Wu et al. (2013). They estimated the maximum detided current speed up to 50 cm s⁻¹, but it included also wind-driven component, which in winter supports flow to the south (Wu et al., 2013).

1410 Offshore, east- or northeastward advected CDW caused by southerly wind, as we observed in 2017, might form detached eddies due to interaction of the Ekman flow and density driven frontal currents (Xuan et al., 2012). Those eddies bring CDW further offshore and alter Physical-physical and -chemical characteristics (including oxygen conditions) and primary production ~~in the water column~~ -eddies can differ significantly from the surrounding water much further from our study area (Wei et al., 2017). On the other hand we noted ventilating impact of colder cyclonic eddy in north in 2015.

1415 Offshore transported CDW occurred simultaneously with coastal upwelling in 2017, as both processes require southerly wind. Shoreward, upslope penetration of the sub-thermocline KSSW-water and hypoxia in the upwelling - CDW interaction-coupling zone (Wei et al., 2017a) were observed. Upwelling, induced by southerly winds and its relaxation supported by northerly winds was captured by cross-sectional in-situ measurements by Yang et al. (2019). Idealized numerical experiment by Liu and Gan (2014) showed that southeasterly wind forcing caused the development of upwelling and shoreward intrusion of colder water in the study area. Wei et al., (2017) showed

1420 how the coupling of the CDW plume front and KSSW upwelling caused DO minimum at the sloping bottom. Likewise N/P ratio and primary production in the CDW is considerably modified by upwelling (Tseng et al., 2014). Phosphate transport by upwelling reduces phosphorus deficiency in the CDW water and therefore promote phytoplankton growth and nitrate uptake (Chen et al., 2004; Zhou et al., 2019).

1425 Time-series of wind displayed large variations in wind forcing ~~on~~ shorter time scales (days to weeks) (Fig. 10) which may alter the stratification pattern and DO distributions considerably. Numerical simulation by Zhang et al. (2018) showed that wind-induced redistribution of the Changjiang river-River bloom-plume changes near-bottom DO conditions rapidly. Also, it has been shown that vertical mixing caused considerable variations in DO concentrations in the near-bottom layer (Ni et al., 2016). In July 2015, 1.5 month before our survey, hypoxia was destroyed-terminated by typhoon, but two days later hypoxic conditions were re-established (Guo et al., 2019).

1430 Our field measurements showed that oxyelineUBD is strongly linked to the thermocline-UBK subsurface water

(Fig. 7). Besides enhanced (or impeded) vertical diapycnal mixing, DO conditions can be altered by vertical movement of isopycnals ~~in this water mass~~. Ni et al. (2016) published a valuable dataset of the time-series DO data in the near-bottom layer. They linked the increase of DO concentrations in the near-bottom layer with the vertical mixing and DO decline in the near-bottom layer with the primary production and consequent decomposition of detritus. One can see several cases from their time-series data (Fig. 2 in Ni et al. (2016)), when near-bottom temperature drops. Those events must be related to the advection of colder water and uplift of the thermocline-KSSW. At the same time, DO declined during those events. Penetration of the cold, low DO water upwards along the coastal slope appear as temperature and DO decline in the point measurement time-series. On the other hand there were some events, where near-bottom layer temperature rises, but sea surface temperature does not change much (e.g. in the beginning of their time-series, Fig. 2 in Ni et al. (2016)). In these cases, DO concentrations increased in the near-bottom layer. Such events can be associated rather to the downward movement of the thermocline or advection of warmer water as we observed in the central section in 2015 (Figs. 4b,e,h,k), than vertical mixing. Thus, vertical location and movement of the thermocline has important role in the near-bottom DO distributions at the coastal slope. Importance of KSSW thickness on the oxygen depletion estimations reveal well also if near bottom oxygen maps are compared with the total AOU maps (Figs. 6g-h). Bottom hypoxia in north in 2017 was much more intense comparing to hypoxia in south in 2015. However, the total AOU was similar in hypoxic zones in both years due to thicker oxygen depleted layer, i.e. thicker KSSW in south in 2015.

Pycnocline dynamics, including downwelling studies, as suggested by Hu and Wang, (2016), are important to investigate in future investigations. Those studies are difficult to arrange with conventional research vessel surveys only. Autonomous measurement platforms, such as are profiling moorings (Lips et al., 2016; Sun et al., 2016), moored sensor chains (Bailey et al., 2019; Venkatesan et al., 2016), which allow capturing the variability in necessary vertical spatio-temporal resolutions can be used. Underwater gliders (Liblik et al., 2016; Rudnick, 2016) might be complicated to use due to strong tidal velocities and heavy ship traffic, but are worthy to consider as well.

Our observations indicated that two physical conditions in the water column must be present for the development of hypoxia. First, high AOU occurred only below thermocline, in the cold KSSW. Secondly, primary production in the fresher CDW or in upwelling is needed to cause high DO consumption that leads to was present in the surface layer when the areas of hypoxia bottoms were observed (Figs. 4-5). Interestingly, these two conditions for hypoxia were valid in very different situations. Shallow (4-6 m) and sharp thermocline coincided with the halocline (related to the CDW) in the northern part of the study area in 2017. Contrary, thermocline and halocline were clearly separated in the southern part of the study area in 2015. Thus, vertical coincidence of halocline and thermocline is not necessary for the hypoxia formation. The thermocline acts as physical barrier, which impedes vertical mixing and DO exchange with upper layers. Primary production in the CDW or in the upwelled water and related DO consumption in the near-bottom layers (Wang et al., 2017, 2016) cause DO decline. Zhu et al (2016) found that the area of DO concentration $< 3.0 \text{ mg l}^{-1}$ fits relatively well fits with the region of the pycnocline strength $> 2.0 \text{ kg m}^{-3}$. This relationship between pycnocline strength and low DO only partly holds truth according to our mappings (Figs. 6a-b, e-f). For instance, there was strong stratification (Fig. 6a) near the river mouth (around 122.5° E and 31° N) in 2015 due to presence of the CDW, but hypoxia was not observed (Fig. 6e) since the colder KSSW was not present. Most of the study area, except very shallow areas had strong enough stratification (pycnocline strength $> 2.0 \text{ kg m}^{-3}$) in 2017 (Fig. 6b). However, hypoxia in the southern part in 2017 was only observed near the coast and in connection to the coastal upwelling (Fig. 6f). Rest of the study area in south was

Formatted: No bullets or numbering

free of hypoxia. In the latter area KSSW was present, but there was no CDW in the surface layer. This means strong stratification as such does not lead necessarily to hypoxia. Two features must be present for hypoxia formation: 1) KSSW, 2) CDW and/or subsurface water upwelling. We can conclude that colder KSSW determines where (including in what depths) hypoxia could develop. Thus, latter provides necessary precondition for hypoxia.

The CDW spreading and/or subsurface water upwelling (and related biogeochemical, biological processes) determine the magnitude, exact location and timing of oxygen depletion. Both features are strongly impacted by wind.

Besides the barrier effect by creation of the thermocline, intrusion of KSSW has other implications on oxygen dynamics. First, the subsurface water is oxygen depleted already before local impact of oxygen consumption. The furthest stations in the southeast (Fig. 1) had AOU of 2-2.5 mg l⁻¹ in the deep layer in 2017, i.e. in the same order that has been estimated in the KSSW before (Qian et al., 2017). The total AOU in the water column there was 50-60 g m⁻² (Fig. 6h). This water is still rather well ventilated comparing to the deep layer waters that had been impacted by upwelling or CDW induced production in the surface layer (Fig. 6g-h). Despite its initial oxygen depletion, Kuroshio intrusion is important source of oxygen import to the study area (Zuo et al., 2019). Without this lateral oxygen advection, hypoxia could form much faster and in larger area (Zuo et al., 2019). Kuroshio intrusion is nutrient rich (Zhang et al., 2007b; Zhou et al., 2019) and in the case of surfacing by its upwelling or vertical mixing could intensify sequence of primary production in the surface, consequently organic matter sinking and producing oxygen consumption in the near-bottom layers.

We have already outlined the main difference in the wind forcing behind formation of the hypoxia in the southern and northern parts of our study area. The one in the north develops under the conditions of summer monsoon. Intense hypoxia can start from very shallow depths (at 5-4-8 m) in the northern area (Fig. 5g) and it can develop very fast under favorable conditions (Guo et al., 2019). On the other hand, hypoxia-bottom layer there can be decay easily due to ventilated by wind stirring or downwelling as we observed at N15 section in 2015 (Fig. 4g). Thus, hypoxia in the northern part can be very pronounced, but disappears fast if forcing changes (Ni et al., 2016). Hypoxia in the southern part of the study area was not so pronounced but quite stable as noted already by Zhu et al. (2011). Continuous decline of the DO from March to October in the southern part was well demonstrated by monthly measurements by Li et al. (2018) (Li et al., 2018b). We suggest three main reasons for this. First, favorable wind conditions for the southward transport are not that frequent in summer. Secondly, the mixture of CDW with ambient ocean water promotes organic matter settling and nutrients consumption on the way to south, so less detritus sinks to the bottom layer and DO consumption is lower in the southern part comparing to the northern counterpart. Third, the KSSW and related thermocline area located deeper in the south is deeper and therefore wind mixing does not destroy the thermocline. In short, the first two reasons account for a lighter hypoxia and the third for a long lasting hypoxia in the southern part.

We have demonstrated that DO conditions off the Changjiang Estuary are sensible to wind forcing. We extracted the wind-climate projection data until 2099 from the Earth System model IPSL-CM5A-MR, but significant changes in the summer monsoon are not foreseen. Thus, future changes in the hypoxia off the Changjiang Estuary could be rather related to the increase in sea surface temperature and consequent extension of the stratified period, and to the intensification of eutrophication.

Formatted: English (United States)

Formatted: Superscript

Conclusions

Two ~~physical-main~~ conditions in the water column must be present for the ~~existence-occurrence~~ of hypoxia in the near-bottom layer off the Changjiang Estuary: ~~thermocline and CDW~~enhanced primary production in the upper layer and KSSW intrusion in the near bottom layer. Pycnocline created by KSSW intrusion is precondition and determines where hypoxia could develop. Primary production in the CDW and/or in the upwelled water, and consequent oxygen consumption by sinking organic matter below pycnocline determine the magnitude, exact location and timing of oxygen depletion. Advection of the CDW and KSSW, likewise occurrence of upwelling, are strongly related to the wind forcing.

Summer monsoon (wind from south) alters CCC by creating Ekman surface flow and by changing the geostrophic current flowing to north or northeast. As a result, the CDW spreads offshore, and KSSW intrudes northwards and upwards on coastal slope, and consequently producing upwelling ~~could occur~~. Joint effect of ~~latter~~these processes can lead to intense and shallow (4-8 m) oxygen depletion ~~connected~~in north and hypoxia at coastal slope in south. Northerly wind intensifies CCC and CDW spreading to south, and causes downwelling. As a consequence, northern part is well ventilated and hypoxia rather occurs further offshore in the southern part.

Wind forcing and river runoff are important contributors of inter-annual variations and annual cycle, determining the size and location of low DO areas. The DO minimum is located more likely in the northern part in July-August and in the southern part during rest of the stratified period.

There is a strong connection between the upper boundaries of KSSW intrusion and oxygen depletion. The sensibility of the boundaries to wind forcing shapes oxygen conditions considerably in the area. Autonomous measurement campaigns by mooring arrays and underwater gliders could considerably improve the knowledge about related processes. Concepts suggested in the present work can be utilized, when planning in-situ experiments. Wind, river discharge, remotely sensed salinity and altimetry data can be used to forecast hydrographic situation and potentially hypoxic areas prior to field works.

~~We found strong correlation between the vertical locations of oxycline (AOU isoline of 2 mg l^{-1}) and thermocline (isotherm $24.5 \text{ }^\circ\text{C}$). Both clines (isolayers) revealed pronounced inclination, being at 50-60 m depth in the southeastern part and near the sea surface in the northern side of the study area.~~

Two very different stratification and DO distributions were registered in the area off the Changjiang Estuary in summers 2015 and 2017. Summer monsoon (wind from south) prevailed and Chinese Coastal Current was altered or even reversed in 2017. The CDW spread mainly to the northeast and east and caused pronounced hypoxic zone in the northern part of the study area. Hypoxic water occupied there most of the water column, as below the CDW at 5-8 m depth strong DO depletion revealed. Another low DO zone, connected to the low saline surface water and upwelled subsurface water, occurred in the southern part of the study area in 2017. According to the long-term wind statistics, this is the prevailing stratification and hypoxia pattern in the area during summers.

Formatted: Not Highlight

Formatted: Tab stops: 3,03 cm, Left

Northerly winds caused intensification of the Chinese Coastal Current and southward transport of the CDW before the survey in 2015. Northern part of the study area was well ventilated, but low DO zone revealed in the southern part. Such a situation occurs if summer monsoon is weaker than long-term average. The two distribution patterns developed by southerly and northerly wind were confirmed by remotely sensed sea surface salinity fields and by circulation simulation. Wind forcing and river runoff are likely main contributors of inter-annual variations determining the size and location of low DO areas. Wind is the main driver of the annual cycle of the lateral DO minimum location. The minimum is located more likely in the northern part in July–August during summer monsoon and in the southern part during rest of the stratified period.

1555

1560

1565 *Code availability.* Scripts to analyze the results are available upon request. Please contact TL.

Author contributions. TL lead the analyzes of the data and writing of the manuscript with contributions of DF and YW. DF was responsible to arrange oceanographic cruises. DS measured chlorophyll *a* in 2015 cruise.

1570 *Competing interests.* We declare that no competing interests are present.

Acknowledgments. This research was funded by the National Natural Science Foundation of China (41776052), Qingdao National Laboratory for Marine Science and Technology (MGQNLN-TD201802), and the Research Fund of State Key Laboratory of Marine Geology at Tongji University (MG20190104).

1575 River data was downloaded from Bulletin of River Sediment in China provided by Ministry of Water Resources of the People's Republic of China (MWR). Website: <http://www.mwr.gov.cn/sj/tjgb/zghlnsgh/> (visited 7th September 2019). We thank Yue Zhang for the gathering the CTD data in 2015, and Junbiao Tu for providing the mooring data, Huiping Xu for agreeing to use their chlorophyll *a* data. We would like to thank our colleagues who helped us in performing measurements. We thank Jaan Laanemets for his comments on the manuscript. We thank reviewer Fabian Große and anonymous reviewer for the valuable comments and suggestions that helped to improve the manuscript.

1580

1585 **References**

Altieri, A. H. and Gedan, K. B.: Climate change and dead zones, *Glob. Chang. Biol.*, 21(4), 1395–1406, doi:10.1111/gcb.12754, 2015.

Association for the Physical Sciences of the Sea, I.: The international thermodynamic equation of seawater-2010: Calculation and use of thermodynamic properties Intergovernmental Oceanographic Commission., 2010.

- 1590 Bailey, K., Steinberg, C., Davies, C., Galibert, G., Hidas, M., McManus, M. A., Murphy, T., Newton, J., Roughan, M. and Schaeffer, A.: Coastal Mooring Observing Networks and Their Data Products: Recommendations for the Next Decade, *Front. Mar. Sci.*, 6, 180, doi:10.3389/fmars.2019.00180, 2019.
- Beardsley, R. C., Limeburner, R., Yu, H. and Cannon, G. A.: Discharge of the Changjiang (Yangtze River) into the East China Sea, *Cont. Shelf Res.*, 4(1–2), 57–76, doi:10.1016/0278-4343(85)90022-6, 1985.
- 1595 Chen, J., Pan, D., Liu, M., Mao, Z., Zhu, Q., Chen, N., Zhang, X. and Tao, B.: Relationships Between Long-Term Trend of Satellite-Derived Chlorophyll-a and Hypoxia Off the Changjiang Estuary, *Estuaries and Coasts*, 40(4), 1055–1065, doi:10.1007/s12237-016-0203-0, 2017.
- Chen, Y.-L. L., Chen, H.-Y., Gong, G.-C., Lin, Y.-H., Jan, S. and Takahashi, M.: Phytoplankton production during a summer coastal upwelling in the East China Sea, *Cont. Shelf Res.*, 24, 1321–1338, doi:10.1016/j.csr.2004.04.002, 2004.
- 1600 Chu, P., Yuchun, C. and Kuninaka, A.: Seasonal variability of the Yellow Sea/East China Sea surface fluxes and thermohaline structure, *Adv. Atmos. Sci.*, 22(1), 1–20, doi:10.1007/BF02930865, 2005.
- Conley, D. J., Björck, S., Bonsdorff, E., Carstensen, J., Destouni, G., Gustafsson, B. G., Hietanen, S., Kortekaas, M., Kuosa, H., Markus Meier, H. E., Müller-Karulis, B., Nordberg, K., Norkko, A., Nürnberg, G., Pitkänen, H., Rabalais, N. N., Rosenberg, R., Savchuk, O. P., Slomp, C. P., Voss, M., Wulff, F. and Zillén, L.: Hypoxia-Related Processes in the Baltic Sea, *Environ. Sci. Technol.*, 43(10), 3412–3420, doi:10.1021/es802762a, 2009.
- 1605 Csanady, G. T.: Circulation in the Coastal Ocean, *Adv. Geophys.*, 23, 101–183, doi:10.1016/S0065-2687(08)60331-3, 1981.
- Cui, Y., Wu, J., Ren, J. and Xu, J.: Physical dynamics structures and oxygen budget of summer hypoxia in the Pearl River Estuary, *Limnol. Oceanogr.*, 64(1), 131–148, doi:10.1002/lno.11025, 2019.
- 1610 Czeschel, R., Schütte, F., Weller, R. A. and Stramma, L.: Transport, properties, and life cycles of mesoscale eddies in the eastern tropical South Pacific, *Ocean Sci.*, 14(4), 731–750, doi:10.5194/os-14-731-2018, 2018.
- Diaz, R. J. and Rosenberg, R.: Spreading dead zones and consequences for marine ecosystems., *Science*, 321(5891), 926–9, doi:10.1126/science.1156401, 2008.
- 1615 Donlon, C. J., Martin, M., Stark, J., Roberts-Jones, J., Fiedler, E. and Wimmer, W.: The Operational Sea Surface Temperature and Sea Ice Analysis (OSTIA) system, *Remote Sens. Environ.*, 116, 140–158, doi:10.1016/J.RSE.2010.10.017, 2012.
- Fofonoff, N. P. and Millard Jr, R. C.: Algorithms for the computation of fundamental properties of seawater., UNESCO. [online] Available from: <https://www.oceanbestpractices.net/handle/11329/109> (Accessed 30 August 2019), 1983.
- 1620 Fong, D. A. and Geyer, W. R.: The Alongshore Transport of Freshwater in a Surface-Trapped River Plume*, *J. Phys. Oceanogr.*, 32(3), 957–972, doi:10.1175/1520-0485(2002)032<0957:TATOFI>2.0.CO;2, 2002.
- Große, F., Fennel, K., Zhang, H. and Laurent, A.: Quantifying the contributions of riverine vs. oceanic nitrogen to hypoxia in the East China Sea, *Biogeosciences Discuss.*, doi:10.5194/bg-2019-342, 2019.
- 1625 Guo, Y., Rong, Z., Li, B., Xu, Z., Li, P. and Li, X.: Physical processes causing the formation of hypoxia off the Changjiang estuary after Typhoon Chan-hom, 2015, *J. Oceanol. Limnol.*, 37(1), 1–17, doi:10.1007/s00343-019-7336-5, 2019.
- Horner-Devine, A. R.: The bulge circulation in the Columbia River plume, *Cont. Shelf Res.*, 29(1), 234–251, doi:10.1016/j.csr.2007.12.012, 2009.
- 1630 Hu, J. and Wang, X. H.: Progress on upwelling studies in the China seas, *Rev. Geophys.*, 54(3), 653–673, doi:10.1002/2015RG000505, 2016.
- Hung, C.-C., Chung, C.-C., Gong, G.-C., Jan, S., Tsai, Y., Chen, K.-S., Chou, W. C., Lee, M.-A., Chang, Y., Chen, M.-H., Yang, W.-R., Tseng, C.-J. and Gawarkiewicz, G.: Nutrient supply in the Southern East China Sea after Typhoon Morakot, *J. Mar. Res.*, 71(1), 133–149, doi:10.1357/002224013807343425, 2013.
- 1635 Kang, Y., Pan, D., Bai, Y., He, X., Chen, X., Chen, C.-T. A. and Wang, D.: Areas of the global major river plumes, *Acta Oceanol. Sin.*, 32(1), 79–88, doi:10.1007/s13131-013-0269-5, 2013.

- Large, W. G. and Pond, S.: Open Ocean Momentum Flux Measurements in Moderate to Strong Winds, *J. Phys. Oceanogr.*, 11(3), 324–336, doi:10.1175/1520-0485(1981)011<0324:OOMFMI>2.0.CO;2, 1981.
- 1640 Lentz, S. J. and Helfrich, K. R.: Buoyant gravity currents along a sloping bottom in a rotating fluid, *J. Fluid Mech.*, 464, 251–278, doi:10.1017/S0022112002008868, 2002.
- Li, D., Jing, Z., Daji, H., Ying, W. and Jun, L.: Oxygen depletion off the Changjiang (Yangtze River) Estuary, *Sci. CHINA (Series D)*, 45(12), 2002.
- Li, L., He, Z., Xia, Y. and Dou, X.: Dynamics of sediment transport and stratification in Changjiang River Estuary, China, *Estuar. Coast. Shelf Sci.*, 213, 1–17, doi:10.1016/J.ECSS.2018.08.002, 2018a.
- 1645 Li, M. and Chen, Z.: An Assessment of Saltwater Intrusion in the Changjiang (Yangtze) River Estuary, China, *Coasts and Estuaries*, 31–43, doi:10.1016/B978-0-12-814003-1.00002-2, 2019.
- Li, M. and Rong, Z.: Effects of tides on freshwater and volume transports in the Changjiang River plume, *J. Geophys. Res.*, 117, 6027, doi:10.1029/2011JC007716, 2012.
- 1650 Li, Y. L.: Seasonal Hypoxia and its Affecting Factors in the Yangtze River Estuary, Ocean University of China, Qingdao (in Chinese), 2015.
- Li, Z., Song, S., Li, C. and Yu, Z.: The sinking of the phytoplankton community and its contribution to seasonal hypoxia in the Changjiang (Yangtze River) estuary and its adjacent waters, *Estuar. Coast. Shelf Sci.*, 208, 170–179, doi:10.1016/J.ECSS.2018.05.007, 2018b.
- 1655 Liblik, T., Karstensen, J., Testor, P., Alenius, P., Hayes, D., Ruiz, S., Heywood, K. J., Pouliquen, S., Mortier, L. and Mauri, E.: Potential for an underwater glider component as part of the Global Ocean Observing System, *Methods Oceanogr.*, 17, 50–82, doi:10.1016/j.mio.2016.05.001, 2016.
- Lie, H.-J. and Cho, C.-H.: Recent advances in understanding the circulation and hydrography of the East China Sea, *Fish. Oceanogr.*, 11(6), 318–328, doi:10.1046/j.1365-2419.2002.00215.x, 2002.
- 1660 Lie, H.-J. and Cho, C.-H.: Seasonal circulation patterns of the Yellow and East China Seas derived from satellite-tracked drifter trajectories and hydrographic observations, *Prog. Oceanogr.*, 146, 121–141, doi:10.1016/J.POCEAN.2016.06.004, 2016.
- Lips, U., Kikas, V., Liblik, T. and Lips, I.: Multi-sensor in situ observations to resolve the sub-mesoscale features in the stratified Gulf of Finland, Baltic Sea, *Ocean Sci.*, 12(3), 715–732, doi:10.5194/os-12-715-2016, 2016.
- 1665 Liu, W., Song, J., Huamao, Y., Li, N., Xuegang, L. I. and Liqin, D.: Dissolved barium as a tracer of Kuroshio incursion in the Kuroshio region east of Taiwan Island and the adjacent East China Sea, *Sci. China Earth Sci.*, 60(7), 1356–1367, doi:10.1007/s11430-016-9039-7, 2017.
- Liu, Z. and Gan, J.: Modeling Study of Variable Upwelling Circulation in the East China Sea: Response to a Coastal Promontory, *J. Phys. Oceanogr.*, 44(4), 1078–1094, doi:10.1175/JPO-D-13-0170.1, 2014.
- 1670 Meissner, T., Wentz, F. J. and Manaster, A.: Remote Sensing Systems SMAP Ocean Surface Salinities [Level 2C, Level 3 Running 8-day, Level 3 Monthly], Version 3.0 validated release. Remote Sensing Systems, Santa Rosa, CA, USA., doi:10.5067/SSSS-TTTT, 2018.
- 1675 Moon, J.-H., Kim, T., Son, Y. B., Hong, J.-S., Lee, J.-H., Chang, P.-H. and Kim, S.-K.: Contribution of low-salinity water to sea surface warming of the East China Sea in the summer of 2016, *Prog. Oceanogr.*, 175, 68–80, doi:10.1016/j.pocean.2019.03.012, 2019.
- Ni, X., Huang, D., Zeng, D., Zhang, T., Li, H. and Chen, J.: The impact of wind mixing on the variation of bottom dissolved oxygen off the Changjiang Estuary during summer, *J. Mar. Syst.*, 154, 122–130, doi:10.1016/j.jmarsys.2014.11.010, 2016.
- 1680 Ning, X., Lin, C., Su, J., Liu, C., Hao, Q. and Le, F.: Long-term changes of dissolved oxygen, hypoxia, and the responses of the ecosystems in the East China Sea from 1975 to 1995, *J. Oceanogr.*, 67(1), 59–75, doi:10.1007/s10872-011-0006-7, 2011.
- Obenour, D. R., Scavia, D., Rabalais, N. N., Turner, R. E. and Michalak, A. M.: Retrospective Analysis of Midsummer Hypoxic Area and Volume in the Northern Gulf of Mexico, 1985–2011, *Environ. Sci. Technol.*, 47(17), 9808–9815, doi:10.1021/es400983g, 2013.

- 1685 Peng, L., Benwei, S., Yaping, W., Weihua, Q., Yangang, L. and Jian, C.: Analysis of the characteristics of offshore currents in the Changjiang (Yangtze River) estuarine waters based on buoy observations, *Acta Ocean. Sin.*, 36(4), 13–20, doi:10.1007/s13131, 2017.
- Qian, W., Dai, M., Xu, M., Kao, S. J., Du, C., Liu, J., Wang, H., Guo, L. and Wang, L.: Non-local drivers of the summer hypoxia in the East China Sea off the Changjiang Estuary, *Estuar. Coast. Shelf Sci.*, 198, 393–399, doi:10.1016/j.ecss.2016.08.032, 2017.
- 1690 Ren, F., Fan, D., Wu, Y. and Zhao, Q.: The evolution of hypoxia off the Changjiang Estuary in the last 3000 years: Evidence from benthic foraminifera and elemental geochemistry, *Mar. Geol.*, 417, 106039, doi:10.1016/J.MARGEO.2019.106039, 2019.
- Rudnick, D. L.: Ocean Research Enabled by Underwater Gliders, *Ann. Rev. Mar. Sci.*, 8(1), 519–541, doi:10.1146/annurev-marine-122414-033913, 2016.
- 1695 Sun, H., Yang, Q., Zhao, W., Liang, X. and Tian, J.: Temporal variability of diapycnal mixing in the northern South China Sea, *J. Geophys. Res. Ocean.*, 121(12), 8840–8848, doi:10.1002/2016JC012044, 2016.
- Testa, J. M. and Kemp, W. M.: Spatial and Temporal Patterns of Winter–Spring Oxygen Depletion in Chesapeake Bay Bottom Water, *Estuaries and Coasts*, 37(6), 1432–1448, doi:10.1007/s12237-014-9775-8, 2014.
- 1700 Tseng, Y.-F., Lin, J., Dai, M. and Kao, S.-J.: Joint effect of freshwater plume and coastal upwelling on phytoplankton growth off the Changjiang River, *Biogeosciences*, 11(2), 409–423, doi:10.5194/bg-11-409-2014, 2014.
- Vaquer-Sunyer, R. and Duarte, C. M.: Thresholds of hypoxia for marine biodiversity., *Proc. Natl. Acad. Sci. U. S. A.*, 105(40), 15452–7, doi:10.1073/pnas.0803833105, 2008.
- 1705 Venkatesan, R., Lix, J. K., Phanindra Reddy, A., Arul Muthiah, M. and Atmanand, M. A.: Two decades of operating the Indian moored buoy network: significance and impact, *J. Oper. Oceanogr.*, 9(1), 45–54, doi:10.1080/1755876X.2016.1182792, 2016.
- Wang, B. and Wang, X.: Chemical hydrography of coastal upwelling in the East China Sea, *Chinese J. Oceanol. Limnol.*, 25(1), 16–26, doi:10.1007/s00343-007-0016-x, 2007.
- 1710 Wang, B., Wei, Q., Chen, J. and Xie, L.: Annual cycle of hypoxia off the Changjiang (Yangtze River) Estuary, *Mar. Environ. Res.*, 77, 1–5, doi:10.1016/j.marenvres.2011.12.007, 2012.
- Wang, B., Chen, J., Jin, H., Li, H., Huang, D. and Cai, W.-J.: Diatom bloom-derived bottom water hypoxia off the Changjiang estuary, with and without typhoon influence, *Limnol. Oceanogr.*, 62(4), 1552–1569, doi:10.1002/lno.10517, 2017.
- 1715 Wang, H., Dai, M., Liu, J., Kao, S.-J., Zhang, C., Cai, W.-J., Wang, G., Qian, W., Zhao, M. and Sun, Z.: Eutrophication-Driven Hypoxia in the East China Sea off the Changjiang Estuary, *Environ. Sci. Technol.*, 50(5), 2255–2263, doi:10.1021/acs.est.5b06211, 2016.
- Wei, Q., Wang, B., Yu, Z., Chen, J. and Xue, L.: Mechanisms leading to the frequent occurrences of hypoxia and a preliminary analysis of the associated acidification off the Changjiang estuary in summer, *Sci. China Earth Sci.*, 60(2), 360–381, doi:10.1007/s11430-015-5542-8, 2017a.
- 1720 Wei, Q., Yu, Z., Wang, B., Wu, H., Sun, J., Zhang, X., Fu, M., Xia, C. and Wang, H.: Offshore detachment of the Changjiang River plume and its ecological impacts in summer, *J. Oceanogr.*, 73(3), 277–294, doi:10.1007/s10872-016-0402-0, 2017b.
- 1725 Weiss, R. F.: The solubility of nitrogen, oxygen and argon in water and seawater, *Deep Sea Res. Oceanogr. Abstr.*, 17(4), 721–735, doi:10.1016/0011-7471(70)90037-9, 1970.
- Wu, H., Deng, B., Yuan, R., Hu, J., Gu, J., Shen, F., Zhu, J., Zhang, J., Wu, H., Deng, B., Yuan, R., Hu, J., Gu, J., Shen, F., Zhu, J. and Zhang, J.: Detiding Measurement on Transport of the Changjiang-Derived Buoyant Coastal Current, *J. Phys. Oceanogr.*, 43(11), 2388–2399, doi:10.1175/JPO-D-12-0158.1, 2013.
- 1730 Wu, Y., Fan, D., Wang, D. and Yin, P.: Increasing hypoxia in the Changjiang Estuary during the last three decades deciphered from sedimentary redox-sensitive elements, *Mar. Geol.*, 106044, doi:10.1016/J.MARGEO.2019.106044, 2019.
- Xu, Q., Zhang, S., Cheng, Y. and Zuo, J.: Interannual Feature of Summer Upwelling around the Zhoushan

- Islands in the East China Sea, *J. Coast. Res.*, 331, 125–134, doi:10.2112/JCOASTRES-D-15-00197.1, 2017.
- 1735 Xu, Z., Ma, J., Wang, H., Hu, Y., Yang, G., Deng, W., Xu, Z., Ma, J., Wang, H., Hu, Y., Yang, G. and Deng, W.: River Discharge and Saltwater Intrusion Level Study of Yangtze River Estuary, China, *Water*, 10(6), 683, doi:10.3390/w10060683, 2018.
- Xuan, J.-L., Huang, D., Zhou, F., Zhu, X.-H. and Fan, X.: The role of wind on the detachment of low salinity water in the Changjiang Estuary in summer, *J. Geophys. Res. Ocean.*, 117(C10), n/a-n/a, doi:10.1029/2012JC008121, 2012.
- 1740 Yang, L., Chen, Z., Sun, Z. and Hu, J.: Sectional characteristics of temperature, salinity and density off the central Zhejiang coast in the spring of 2016, *Acta Oceanol. Sin.*, 38(4), 175–182, doi:10.1007/s13131-019-1421-7, 2019.
- Ye, W., Zhang, G., Zhu, Z., Han, Y., Wang, L. and Sun, M.: Methane distribution and sea-to-air flux in the East China Sea during the summer of 2013: Impact of hypoxia, *Deep Sea Res. Part II Top. Stud. Oceanogr.*, 124, 74–83, doi:10.1016/J.DSR2.2015.01.008, 2016.
- 1745 Zhang, J., Liu, S. M., Ren, J. L., Wu, Y. and Zhang, G. L.: Nutrient gradients from the eutrophic Changjiang (Yangtze River) Estuary to the oligotrophic Kuroshio waters and re-evaluation of budgets for the East China Sea Shelf, *Prog. Oceanogr.*, 74(4), 449–478, doi:10.1016/j.pocean.2007.04.019, 2007a.
- 1750 Zhang, L., Liu, Z., Zhang, J., Hong, G. H., Park, Y. and Zhang, H. F.: Reevaluation of mixing among multiple water masses in the shelf: An example from the East China Sea, *Cont. Shelf Res.*, 27(15), 1969–1979, doi:10.1016/J.CSR.2007.04.002, 2007b.
- Zhang, W., Wu, H. and Zhu, Z.: Transient Hypoxia Extent Off Changjiang River Estuary due to Mobile Changjiang River Plume, *J. Geophys. Res. Ocean.*, 123(12), 9196–9211, doi:10.1029/2018JC014596, 2018.
- 1755 Zhang, W., Wu, H., Hetland, R. D. and Zhu, Z.: On Mechanisms Controlling the Seasonal Hypoxia Hot Spots off the Changjiang River Estuary, *J. Geophys. Res. Ocean.*, 2019JC015322, doi:10.1029/2019JC015322, 2019.
- Zhou, Z., Yu, R., Sun, C., Feng, M. and Zhou, M.: Impacts of Changjiang River Discharge and Kuroshio Intrusion on the Diatom and Dinoflagellate Blooms in the East China Sea, *J. Geophys. Res. Ocean.*, 124(7), 2019JC015158, doi:10.1029/2019JC015158, 2019.
- 1760 Zhu, J., Zhu, Z., Lin, J., Wu, H. and Zhang, J.: Distribution of hypoxia and pycnocline off the Changjiang Estuary, China, *J. Mar. Syst.*, 154, 28–40, doi:10.1016/j.jmarsys.2015.05.002, 2016.
- Zhu, Z.-Y., Zhang, J., Wu, Y., Zhang, Y.-Y., Lin, J. and Liu, S.-M.: Hypoxia off the Changjiang (Yangtze River) Estuary: Oxygen depletion and organic matter decomposition, *Mar. Chem.*, 125(1–4), 108–116, doi:10.1016/J.MARCHEM.2011.03.005, 2011.
- 1765 Zhu, Z. Y., Wu, H., Liu, S. M., Wu, Y., Huang, D. J., Zhang, J. and Zhang, G. Sen: Hypoxia off the Changjiang (Yangtze River) estuary and in the adjacent East China Sea: Quantitative approaches to estimating the tidal impact and nutrient regeneration, *Mar. Pollut. Bull.*, 125(1–2), 103–114, doi:10.1016/j.marpolbul.2017.07.029, 2017.
- 1770 Zuo, J., Song, J., Yuan, H., Li, X., Li, N. and Duan, L.: Impact of Kuroshio on the dissolved oxygen in the East China Sea region, *J. Oceanol. Limnol.*, 37(2), 513–524, doi:10.1007/s00343-019-7389-5, 2019.

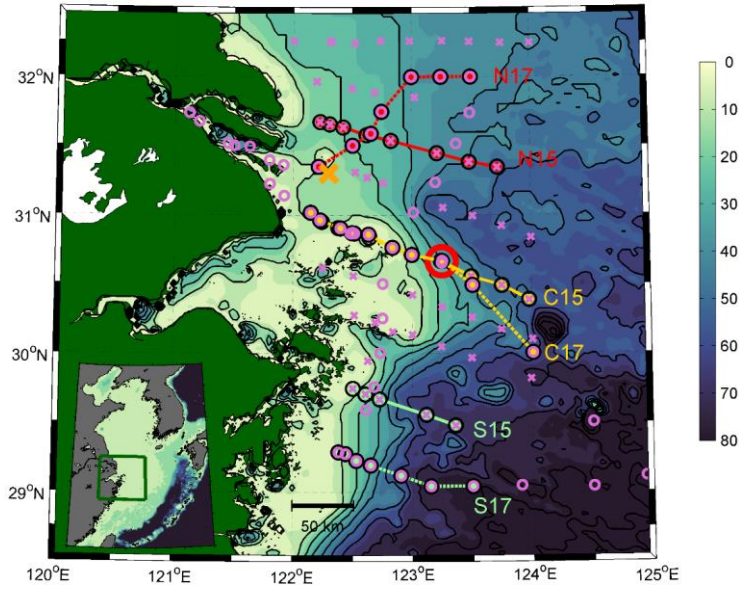


Figure 1. Map of the study area off the Changjiang Estuary. Purple crosses represent CTD cast stations conducted on 27 August – 5 September in 2015 and purple circles show CTD cast stations on 24 - 29 July in 2017. Red lines represent northerly sections (N15 in 2015 and N17 in 2017), yellow lines central sections (C15 in 2015 and C17 in 2017), and green lines southern sections (S15 in 2015 and S17 in 2017). Larger red circle represents the mooring M1 location. Orange cross shows the location, where wind data were gathered. Color scale shows depth (m) of the study area. The inlay shows the study area in the East China Sea.

1775

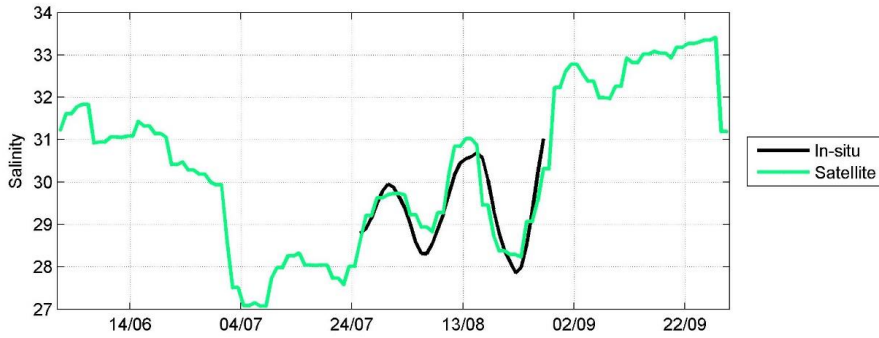


Figure 2. Time-series of in-situ and remotely sensed 8-day running mean salinity at the M1 location in 2017.

1780

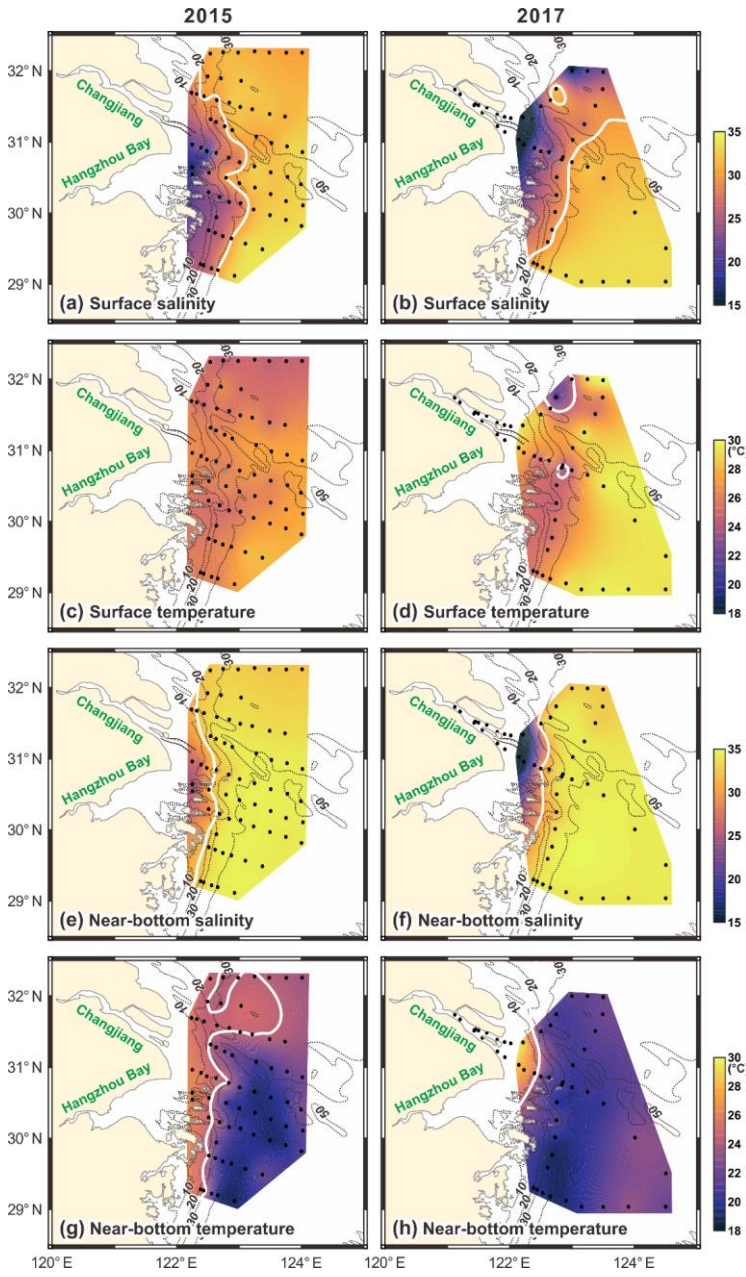


Figure 3. Maps of surface salinity (a, b), surface temperature (c, d), near-bottom salinity (e, f) and near-bottom temperature (g, h) from the surveys in 2015 (left panel) and 2017 (right panel). 24.5 °C and 30.1 psu isolines are shown as white lines.

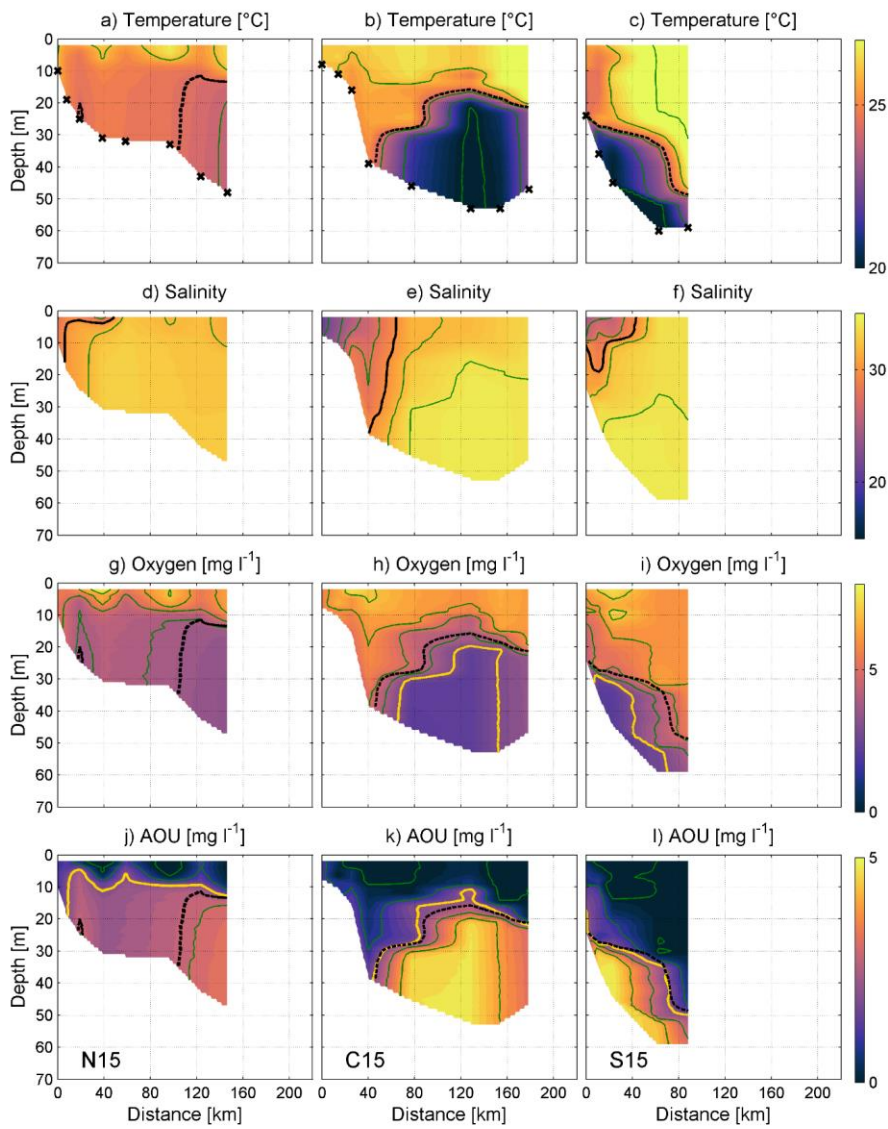
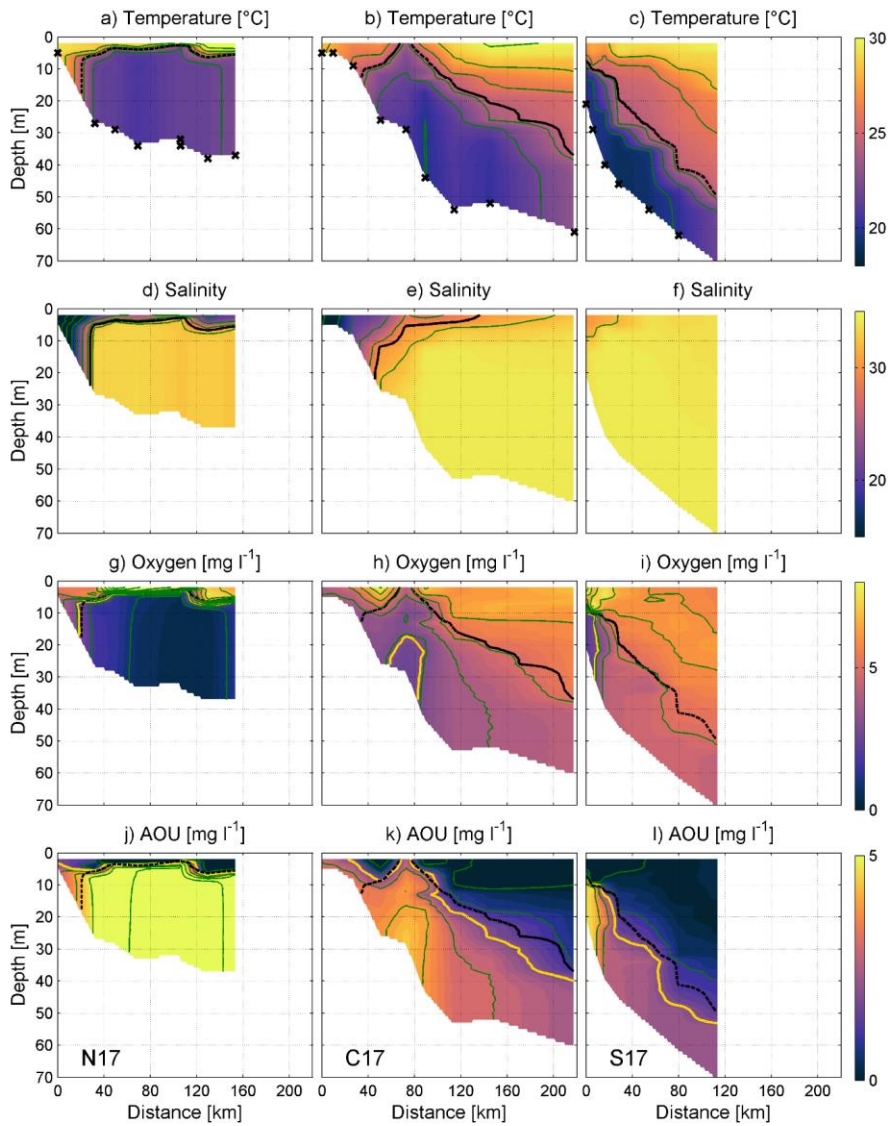


Fig. 4. Vertical distributions of temperature, salinity, density, DO concentration, and Apparent Oxygen Utilization (AOU) along sections N15, C15, and S15 in 2015 (Fig. 1). Temperature isoline 24.5 °C is shown with thicker dashed black line in the temperature, oxygen and AOU plots. AOU isoline 2 mg l⁻¹ is shown with thicker solid yellow-black line in AOU plots. Hypoxia border (3.0 mg l⁻¹) is shown with thicker solid white-line in oxygen plots. Thin lines represent isolines of temperature with 2 °C step, salinity with 2 step, oxygen and AOU with 2 mg l⁻¹ step both. Locations of CTD stations are shown as crosses in the top panels. Values on the x-axis indicate the distance from the westernmost point of a section (Fig. 1).



805

Fig. 5. Vertical distributions of temperature, salinity, density, DO concentration and AOU along sections N17, C17, S17 in 2017 (Fig. 1). Temperature isoline 24.5 °C and AOU isoline 2 mg l⁻¹ (upper panels) are shown with solid black line. Hypoxia border (3.0 mg l⁻¹) is shown with solid white line. Temperature isoline 24.5 °C is shown with dashed line in the temperature, oxygen and AOU plots. AOU isoline 2 mg l⁻¹ is shown with solid line in AOU plots. Hypoxia border (3.0 mg l⁻¹) is shown with solid line in oxygen plots. Locations of CTD stations are shown as crosses in the top panels. Thin lines represent isolines of temperature with 2 °C step, salinity with 2 step, oxygen and AOU with 2 mg l⁻¹ step both. Values on the x-axis indicate the distance from the westernmost point of a section (Fig. 1).

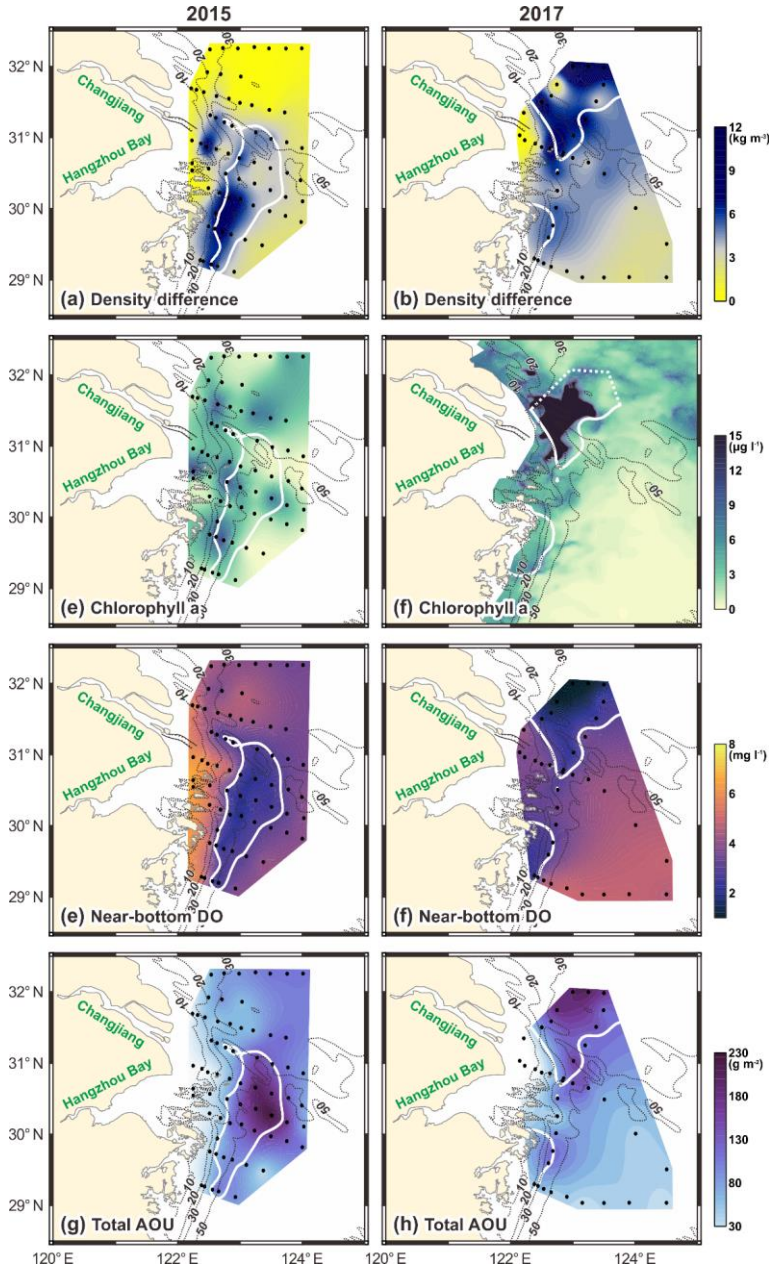


Fig 6. Maps of density difference between the near-bottom layer and surface layer (a,b), in-situ Chl *a* (c), satellite derived Chl *a* (d), near-bottom DO (mid-panel e,f) and total AOU in the water column (g,h) (lowest panel). Maps of in 2015 are shown on left panels (left) and 2017 on (right). Remotely sensed Chl *a* map (f) is a mean field of two daily images of 21-22 July. AOU was calculated according to Eq. (3) Only positive values of AOU were used in the vertical integration of the AOU profile.

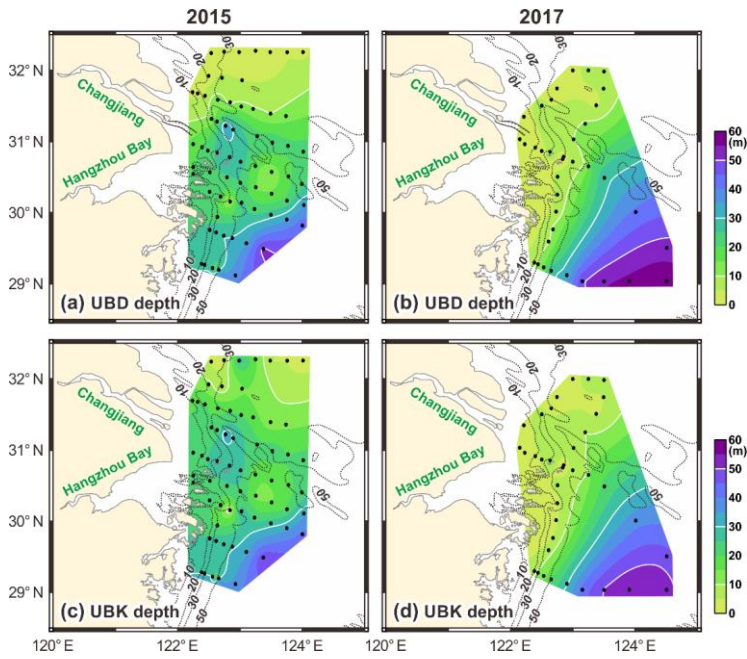
Formatted: Left, Don't adjust space between Latin and Asian text, Don't adjust space between Asian text and numbers

Formatted: Font: 9 pt, Bold

Formatted: Font: (Default) Times New Roman, 9 pt, Bold

Formatted: Font: (Default) Times New Roman, 9 pt

Formatted: Font: 9 pt, Not Bold, Font color: Auto, Estonian



1815

Fig. 7. Maps of AOU isopleth 2 mg l⁻¹ (UBD) depth (upper panels) and temperature isopleth 24.5 °C (UBK) depth (lower panels) in 2015 (left panels) and in 2017 (right panels).

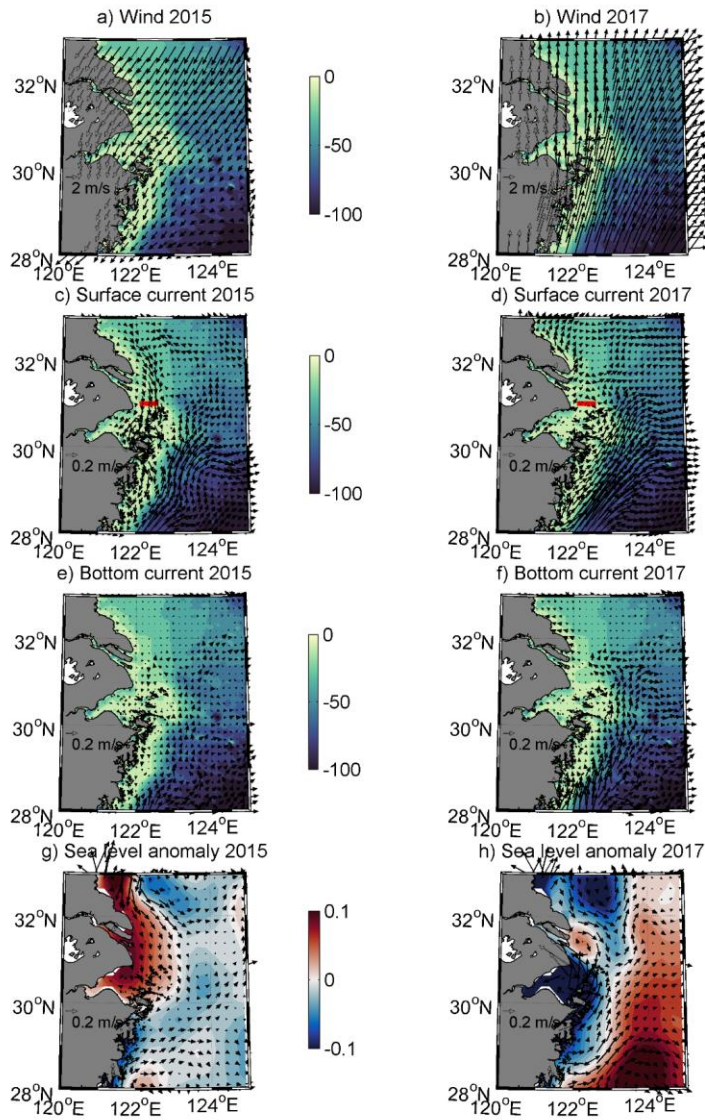
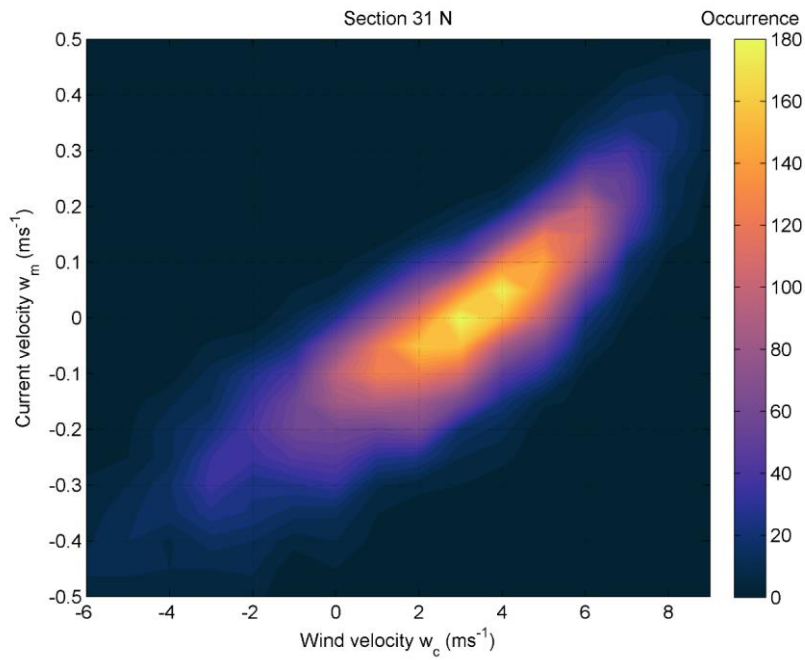


Figure 8. Maps of mean wind (panels a-b, ms^{-1}), simulated surface current (panels c-d, cms^{-1}) and bottom current (e-f, cms^{-1}) s currents in the sea bottom depths down to 100 m during 7 days period prior to the CTD surveys. Bottom bathymetry is shown as a background in panels a-f. Red lines in panels c and d show the section S1, where current time-series (presented in Fig. 10c) were calculated. Every fourth current vector is shown only in the panels c-f. **Persistent current in the southeastern side is the Taiwan Warm Current.** Mean sea level anomaly (m) as contours and geostrophic velocities (cms^{-1}) as vectors derived from satellite altimetry during the surveys are shown in the panels g-h.



1825

Figure 9. Relation of daily mean SE-NW wind velocity component w_c (positive towards NW) and meridional current velocity component w_m (positive northward) in the section at 31° (section S1 in Fig. 8) in 1993-2018. Wind speed steps of 1 m s^{-1} for wind velocity component and 0.05 m s^{-1} for current velocity component were used to calculate histogram. Color scale shows the co-occurrence (number of cases) of respective wind velocity and current velocity component combinations.

1830

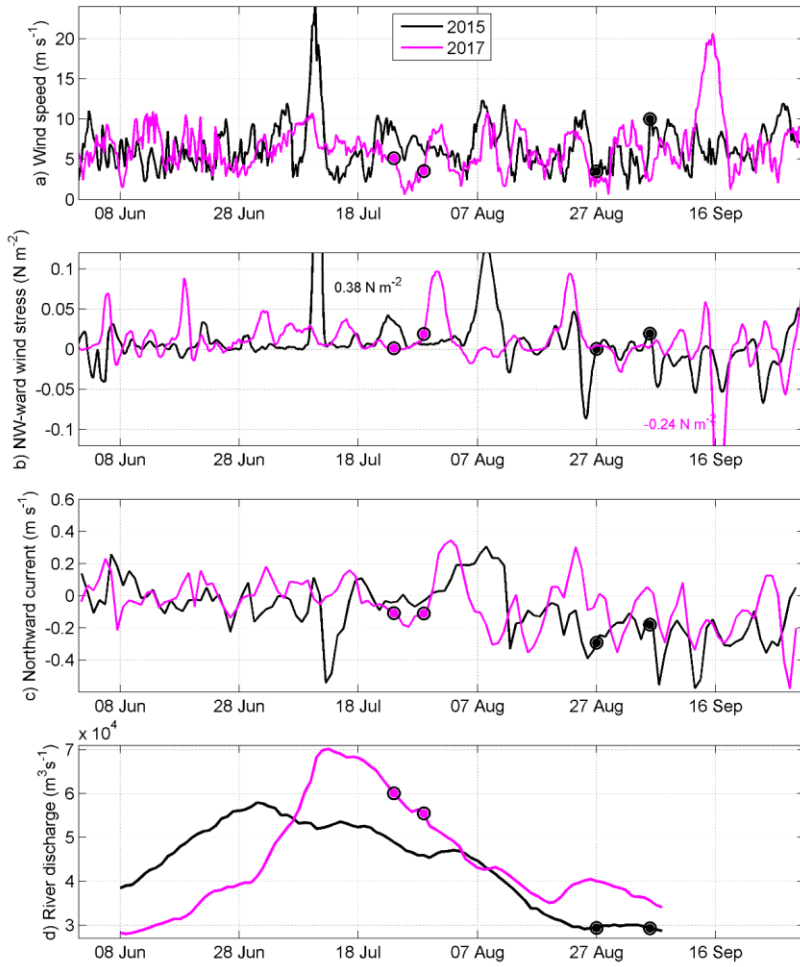


Figure 10. Time-series of wind, current, and river discharge. Mean wind speed (6-hours) (a), 1-day running mean SE-NW wind stress τ_e (positive towards NW; N m^{-2}) (b), daily mean meridional current velocity component v_m (positive northward) at section S1 (c), and daily Changjiang river discharge at Datong station shifted by 7 days to represent flow in the river mouth (d). Blue and red dots represent start and end of the CTD surveys, respectively in 2015 and 2017.

1835

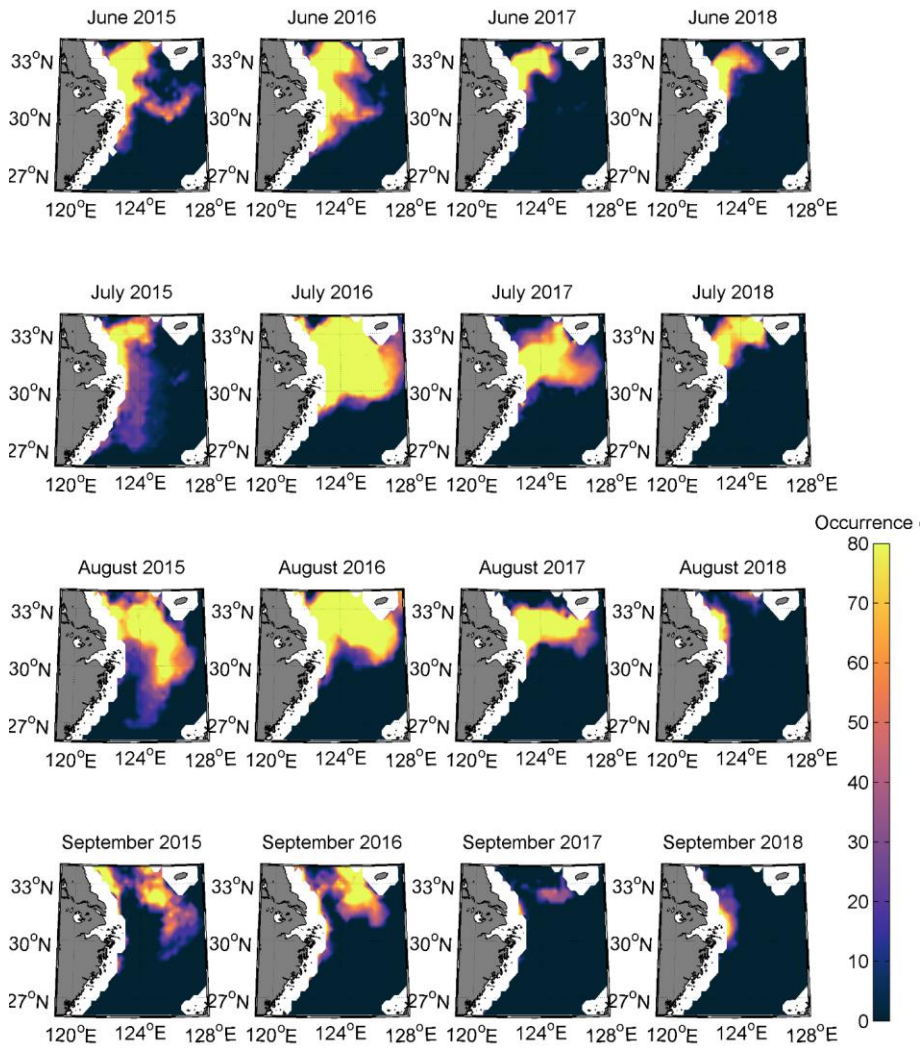


Figure 11. Maps of monthly occurrence (%) of (remotely sensed) salinity $< 30 \text{ g kg}^{-1}$ from June to September, 2015-2018.

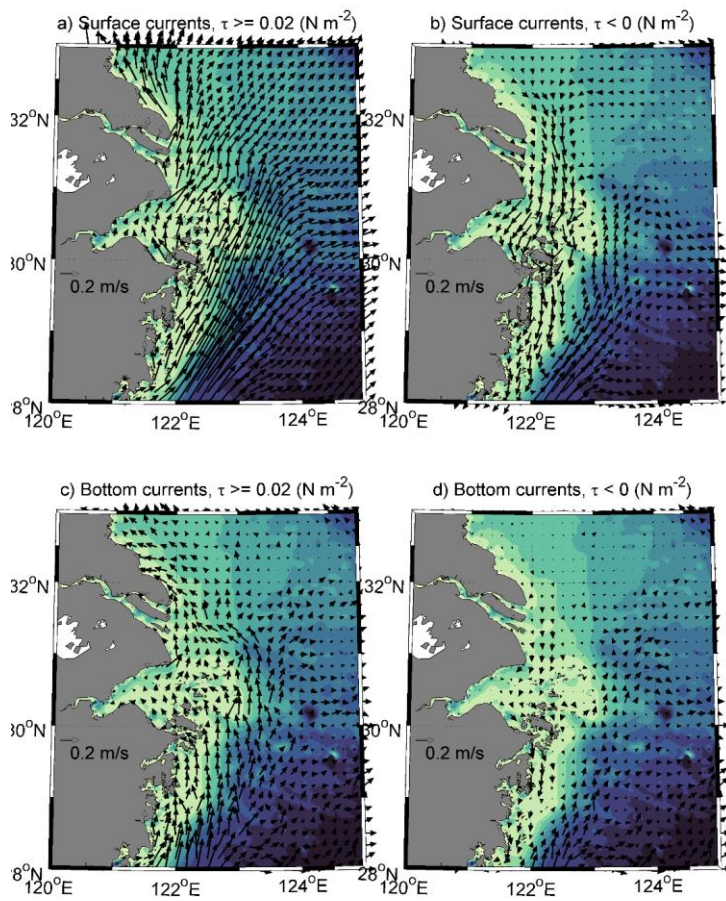
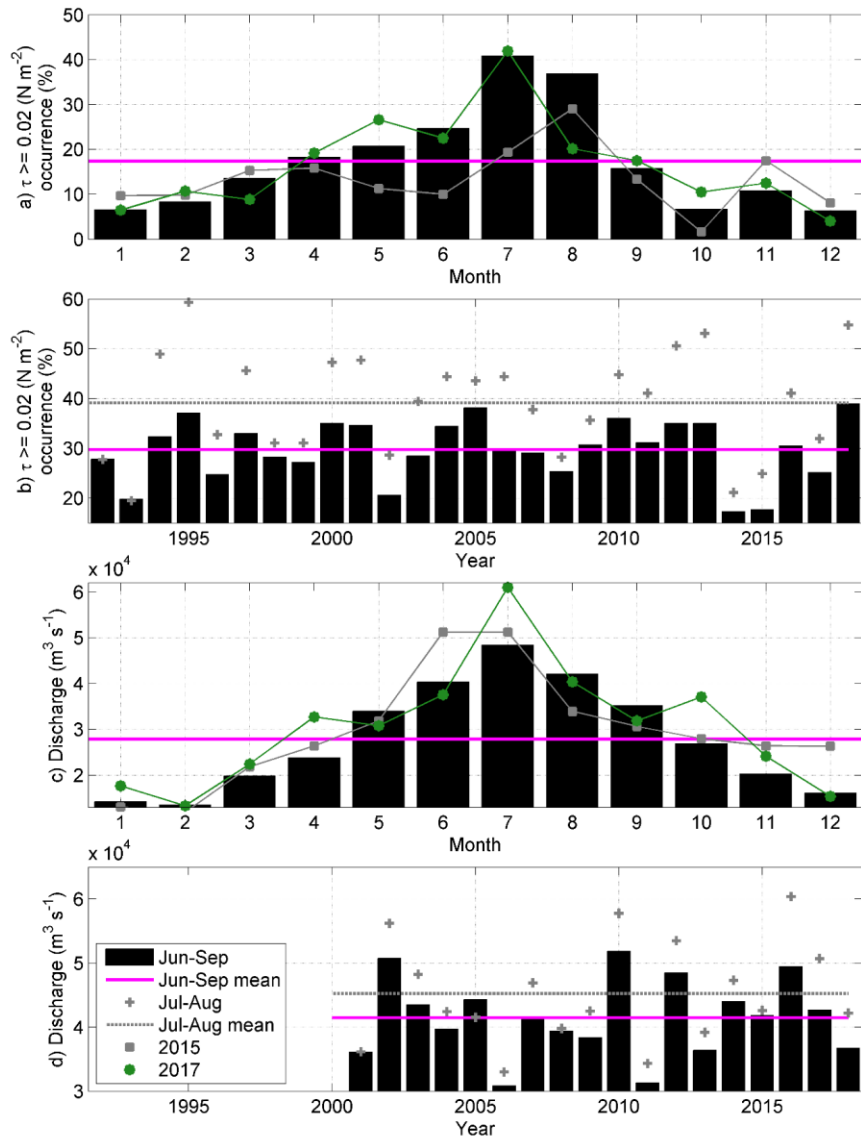


Figure 12. Maps of surface (upper panels) and near-bottom (lower panels) currents in the sea bottom depths down to 100 m in the cases of wind stress component $\tau_c \geq 0.02 \text{ N m}^{-2}$ (left panels) and $\tau_c < 0 \text{ N m}^{-2}$ (right panels) in 1993-2018. Every fourth current vector is shown.



1845

Figure 13. Annual cycle (a, c) and inter-annual variability (b, d) of wind stress component (1992-2018) $\tau_c \geq 0.02 \text{ N m}^{-2}$ (a, b) and river discharge (c, d) (2001-2018). Blue line shows the overall mean in (a) and (c), and June-September long-term mean in (c) and (d). Red line shows the July-August long-term mean in (b) and (d).

1850

Table 1. Summary of general features observed in the study area in summers 2015 and 2017

Summer 2015	Summer 2017
Southward transport of the CDW	East/northeastward transport of the CDW
Stronger stratification in the south	Stronger stratification in the north
Generally lower SST	Generally higher SST
No low DO concentration zone in the north <u>Downwelling along the coast</u>	Strong and shallow hypoxic zone in the north <u>Upwelling along the coast</u>
Bottom water warmer and fresher in the north <u>Higher Chl <i>a</i> in south</u>	Bottom water colder and saltier in the north <u>Higher Chl <i>a</i> in north</u>
No low DO concentration zone in the north Lower DO concentrations further offshore at sea depths ≥ 30 m in the south	Strong and shallow hypoxic zone in the north Lower DO concentrations in the coastal upwelling zone in the south
Bottom water warmer and fresher in the north	Bottom water colder and saltier in the north
Lower DO concentrations further offshore at sea depths ≥ 30 m in the south	Lower DO concentrations in the coastal upwelling zone in the south

Formatted: Estonian

Formatted: Estonian